PROJECT PROGRESS TRACKING USING LIDAR AND 4D DESIGN MODELS

Final Report

SPR 811

Oregon Department of Transportation

PROJECT PROGRESS TRACKING USING LIDAR AND 4D DESIGN MODELS

Final Report

SPR 811

by

Yelda Turkan
Michael J. Olsen
John Gambatese
Nisha Puri

Oregon State University
Kearney Hall, Corvallis, OR 97331

for

Oregon Department of Transportation
Research Section
555 13th Street NE, Suite 1
Salem OR 97301

and

Federal Highway Administration
1200 New Jersey Ave. SE
Washington, DC 20590-0003

June 2019

Technical Report Documentation Page

1. Report No.	2. Government Accession No.	3. Recipient's Catalog No.
FHWA-OR-RD-19-12		

4. Title and Subtitle	5. Report Date
Project Progress Tracking Using Lidar and 4D Design Models	June 2019
	6. Performing Organization Code

7. Author(s)	8. Performing Organization Report No.
Yelda Turkan, Michael J. Olsen, John Gambatese, and Nisha Puri	

9. Performing Organization Name and Address	10. Work Unit No. (TRAIS)
Oregon Department of Transportation Research Section 555 13th Street NE, Suite 1 Salem, OR 97301	11. Contract or Grant No. SPR 811

12. Sponsoring Agency Name and Address	13. Type of Report and Period Covered
Oregon Dept. of Transportation Research Section 555 13th Street NE, Suite 1 Salem, OR 97301 Federal Highway Admin. 1200 New Jersey Ave. SE Washington, DC 20590-0003	Final Report
	14. Sponsoring Agency Code

15. Supplementary Notes

16. Abstract: Accurate data collected from on-going construction projects assists project field engineers with tracking the progress of construction work. The comparison of as-planned schedules against the as-built status of construction enables the involved parties to determine project performance. Periodic monitoring of project performance enables timely identification of discrepancies between the schedule baseline and project schedule. The rapid identification of discrepancies allows necessary measures to be taken to minimize the impact of a delay on the construction workflow. In transportation projects, the traditional means of acquiring as-built data from a construction site prevents involved parties from receiving the required information from the site in a timely manner. The delay in the communication of information ultimately causes subsequent delays in implementing necessary courses of action targeted toward improving the workflow. Therefore, this project develops a technology-supplemented progress monitoring approach. The technology accurately records as-built data with a high level of detail from a construction worksite within a reasonable period of time using lidar while ensuring the safety of the data collector. The proposed framework utilizes point cloud data obtained using mobile lidar technology and 4D Design Models to identify deviations of the performed work from the planned work. Percentage of Completion (POC) for the as-built bridge elements are calculated and compared with the as-planned POC. The differences between these two POC values for an element, on a particular scan date, are used for assessing the performance of the proposed framework.

17. Key Words	18. Distribution Statement
Construction progress tracking, mobile lidar, 4D Design Models, Object Recognition System	Copies available from NTIS, and online at www.oregon.gov/ODOT/Programs/Pages/Research-Publications.aspx

19. Security Classification (of this report): Unclassified	20. Security Classification (of this page): Unclassified	21. No. of Pages	22. Price
		80	

SI* (MODERN METRIC) CONVERSION FACTORS

APPROXIMATE CONVERSIONS TO SI UNITS

Symbol	When You Know	Multiply By	To Find	Symbol
		LENGTH		
in	inches	25.4	millimeters	mm
ft	feet	0.305	meters	m
yd	yards	0.914	meters	m
mi	miles	1.61	kilometers	km
		AREA		
in^2	square inches	645.2	millimeters squared	mm^2
ft^2	square feet	0.093	meters squared	m^2
yd^2	square yards	0.836	meters squared	m^2
ac	acres	0.405	hectares	ha
mi^2	square miles	2.59	kilometers squared	km^2
		VOLUME		
fl oz	fluid ounces	29.57	milliliters	ml
gal	gallons	3.785	liters	L
ft^3	cubic feet	0.028	meters cubed	m^3
yd^3	cubic yards	0.765	meters cubed	m^3
~NOTE: Volumes greater than 1000 L shall be shown in m^3.				
		MASS		
oz	ounces	28.35	grams	g
lb	pounds	0.454	kilograms	kg
T	short tons (2000 lb)	0.907	megagrams	Mg
		TEMPERATURE (exact)		
°F	Fahrenheit	(F-32)/1.8	Celsius	°C

APPROXIMATE CONVERSIONS FROM SI UNITS

Symbol	When You Know	Multiply By	To Find	Symbol
		LENGTH		
mm	millimeters	0.039	inches	in
m	meters	3.28	feet	ft
m	meters	1.09	yards	yd
km	kilometers	0.621	miles	mi
		AREA		
mm^2	millimeters squared	0.0016	square inches	in^2
m^2	meters squared	10.764	square feet	ft^2
m^2	meters squared	1.196	square yards	yd^2
ha	hectares	2.47	acres	ac
km^2	kilometers squared	0.386	square miles	mi^2
		VOLUME		
ml	milliliters	0.034	fluid ounces	fl oz
L	liters	0.264	gallons	gal
m^3	meters cubed	35.315	cubic feet	ft^3
m^3	meters cubed	1.308	cubic yards	yd^3
		MASS		
g	grams	0.035	ounces	oz
kg	kilograms	2.205	pounds	lb
Mg	megagrams	1.102	short tons (2000 lb)	T
		TEMPERATURE (exact)		
°C	Celsius	1.8C+32	Fahrenheit	°F

*SI is the symbol for the International System of Measurement

ACKNOWLEDGEMENTS

The authors would like to thank the Oregon Department of Transportation (ODOT) for funding this research. The authors thank the members of the ODOT Project Technical Advisory Committee Steven Cooley, Christopher Pucci, Ray Thwaits, Thomas Feeley and Chris Bucher, and Norris Shippen from ODOT Research, for their support. The authors would also like to thank Andrew Senogles, Erzhuo Che, Marion Jamieson and Wiley Ferron for their help with data collection. Leica Geosystems provided software utilized in this study.

DISCLAIMER

TABLE OF CONTENTS

LIST OF TABLES

LIST OF FIGURES

1.0 INTRODUCTION

Systematic collection of accurate and detailed data from on-going construction projects is important for monitoring project progress. The acquired data can be processed to generate information about the status of completion of various activities. This information can be used by various parties involved in the project for decision-making and to find effective solutions to overcome any delays. Timely identification of construction delays is possible if such information is collected frequently and with sufficient detail from the construction site.

The first chapter of this report, for the "Project Progress Tracking Using Lidar and 4D Design Models" study, provides the background and objectives of the study. The next chapter reviews the current literature on the various technologies that are used in the construction industry, with a specific focus on the technologies that are used for progress tracking. Chapters 3 and 4 detail the experimental design and research methodology respectively. Chapter 5 provides the data analysis and results. Finally, the report concludes with a discussion on the limitations and provides suggestions for expanding the project further in future work.

1.1 BACKGROUND

The investment in transportation infrastructure in the United States is estimated to reach $278.1 billion in 2019 (*American Road & Transportation Builders Association 2017*). Every four years, the American Society of Civil Engineers (ASCE) releases a comprehensive assessment of the U.S. infrastructure as a "report card". The most recent report card that ASCE published in 2017 issued an overall grade of D+ (poor) for the nation's infrastructure, and C+ (mediocre) for bridges. The report estimated that 188 million trips were taken daily across deteriorating roads, bridges and highways (*Economic Development Research Group et al, 2016*). Based on their assessment, the current state of transportation infrastructure resulted in increased travel times and a number of accidents on roads (*Economic Development Research Group et al, 2016*). Ultimately, these conditions has a negative impact on the cost of delivered goods and personal income (*Economic Development Research Group et al, 2016*).

Frequent inspection of existing transportation infrastructure and performing necessary repair work in a timely manner can ensure good conditions of roads and bridges. In addition to performing comprehensive inspections regularly after the construction phase, proper measures implemented during the construction phase also help ensure good quality. During the pre-construction phase, the various parties involved in a project collectively define the milestones of the project based on the expected duration of completion and the available budget. Under the constant pressure of completing the required work within a given time period while monitoring the available budget, the quality of work performed may be compromised (*Nee 1996*). In addition, failure to communicate the project performance with all involved parties in an effective and timely manner may lead to delays and cost-overruns in construction work (*Owolabi et al., 2014*).

Transportation construction projects often experience significant cost overruns and schedule delays (*Bhargava et al. 2010; Cantarelli et al., 2010; Flyvbjerg et al., 2003*). Obtaining reliable progress information pertaining to on-site activities would enable identifying issues that can cause delays in the completion of these activities. Progress information acquired using current manual-based progress measurement workflows are prone to errors and are time consuming (*Vick and Brilakis 2016*). Additionally, multiple site visits may be required if the collected data is inaccurate or incomplete. Therefore, the inefficiencies associated with manual-based progress measurement methods indicates the need for adopting new technologies for project progress monitoring.

In this study, a novel project progress tracking framework that uses lidar data and four-dimensional (4D) Design Models (3D design model + project schedule) was developed. A 4D model is obtained when 3D design model elements are linked to project schedule. A 4D model linked to project cost information is referred to as a 5D project model (*Schneider 2013*). Lidar creates a digital snapshot of the project site scanned, which can provide not only timely information about the construction progress, but also a detailed record of the construction process that can be repeatedly queried, as needed. The next chapter of this report reviews project progress tracking practices both in transportation and the building construction industry. It is worth noting that the use of lidar and advanced technologies are much more mature for building construction projects than for transportation projects, and some of these techniques may be adapted or help inform processes developed for transportation projects, which is why they are included in this report. Moreover, the concepts and technologies adopted for monitoring the progress in building construction projects are applicable to transportation construction projects as well. However, the application of such technologies and concepts still needs to be evaluated. Types of technologies that have been adopted for progress monitoring purposes are also discussed in the next chapter, which includes the current initiatives and uses of 4D design models, lidar, and several other technologies in the transportation industry as well as by ODOT.

1.2 GOAL AND OBJECTIVES OF THE STUDY

Previous studies have developed frameworks for project progress tracking, specifically designed for building construction projects. The goal of this study is to design a progress tracking framework that can be used by ODOT to better monitor the progress of horizontal (or heavy civil) construction projects, bridge construction projects in particular, and make timely decisions when necessary. To meet this goal, the following objectives were defined for this study:

1. Develop a framework that reports the progress of each construction element in horizontal construction projects in the form of Percentage of Completion (POC).

2. Test and validate the framework using a real-life case study, and investigate the framework's applicability in tracking the progress of horizontal construction projects.

1.3 RESEARCH TASKS AND METHODS

To meet the project goal and the stated objectives, five primary research tasks have been identified that are detailed below.

1.3.1 Literature Review

To identify the existing gaps in knowledge, the state-of-the-art progress tracking practices in the horizontal and vertical construction industry were investigated. These findings are summarized in Chapter 2. For this work, a comprehensive search of archival publications was performed to facilitate this research task. All articles and publications relevant to the theme of this research were analyzed to identify gaps in the existing body of knowledge. The identified gaps serve as guidelines for designing the proposed framework. In addition, the various types of technologies used in progress tracking of construction projects in both industry and academia were identified. The comparison between the characteristics of these technologies was performed to obtain a basic understanding regarding the performance of these technologies in progress tracking. The characteristics include the accuracy of data collected, data analysis procedures, installation and setup times, mobility of associated equipment and the location of projects that are best suited for implementing these technologies (indoor or outdoor). Furthermore, the comparison of different lidar platforms for project progress tracking was performed. Different characteristics, such as 3D position accuracy, resolution, cost, data pre-processing and equipment setup were compared between these platforms. Furthermore, the adoption of BIM for Infrastructure practices in the transportation industry, in general, as well as within the Oregon Department of Transportation (ODOT) were discussed.

1.3.2 Research Methodology

The research methodology includes identification of the technologies or data collection platforms to be used for acquiring as-built data. A site suitable for data collection was selected for collecting data from the construction site periodically. The challenges regarding data collection were identified and their impact on data collection and the quality of data collected are discussed.

Based on the literature review, a progress tracking framework was developed. The framework involves a series of steps for processing the collected data to output progress tracking results that describe the performance of a project on a given date. The steps involve data preprocessing, data processing including coarse and fine registration steps between as-built and virtual point cloud data, segmentation and object recognition, and POC calculation. A case study was then used to validate the proposed framework. Algorithms and methods designed during this process, including the validation results, are included in this report.

1.3.3 Data Collection

The data for this study was collected as detailed in Section 3.1. In summary, in this study as-built data was collected using a TOPCON IP-S2 mobile lidar mapping system from a small bridge construction project located in Albany, OR. A 3D design model of the bridge was developed manually by the research team using the 2D design drawings that were provided. All data was recorded in a standardized and secure form and will be delivered to ODOT with the final version of this report.

1.3.4 Data Analysis (Validation of Framework)

The collected data will be analyzed using the methods discussed in Section 1.3.2. The time required for performing each of the steps is presented to help ODOT implement this technology for project progress tracking. The results obtained using this workflow will assist ODOT personnel with decision making and prioritizing project tasks.

1.4 BENEFITS

The developed semi-automated progress tracking framework utilizes highway construction as-built data and 4D design models to evaluate the status of construction. Acquisition of as-built data on a regular basis would enable project stakeholders to effectively prepare solutions that would help bring the project back on track. It also fosters speedy and effective communication among project stakeholders, which enables proposed solutions to be implemented efficiently.

Thus, the periodic collection and analysis of as-built data contributes toward the completion of the project by avoiding possible delays, which would otherwise result from ineffective and delayed communication. This study proposes a progress tracking framework for bridge construction projects that accurately tracks the progress of construction. The results obtained using this workflow will help ODOT personnel with decision making and prioritizing project tasks.

1.5 IMPLEMENTATION

The final product of this project is the progress tracking framework, which includes codes for algorithms designed in the process, as well as this report that describes the details of the framework. ODOT will ensure the final product of the study is available online so that the framework can be used by state transportation agencies and DOTs for tracking the progress of horizontal construction projects.

2.0 LITERATURE REVIEW

Monitoring the progress of an on-going construction project starts with the development of a work plan that dictates how the project will progress and meet the established objectives. Progress measures and metrics for each activity show the cost and time associated with the completion of the activity. At the beginning of the progress monitoring cycle, as-built data is acquired from the site and the work performed is measured using information from the costs incurred to date and the volumetric work calculations. This information, along with its comparison against as-planned work, is then reported to involved parties. Based on the current progress, a forecast for the project completion date is also reported. Problems that have occurred or topics relevant to performing the work on-site are discussed and necessary actions are taken. As these issues are addressed, their potential impact on the duration of the entire project is determined *(Arcuri 2007)*. Several studies have focused on implementing a variety of technologies including nD (3D, 4D and 5D) models, lidar, radio frequency identification (RFID) tags, and Ultra-wideband (UWB) sensors for progress monitoring both in building and transportation construction projects.

2.1 TECHNOLOGIES USED IN TRACKING BUILDING CONSTRUCTION PROJECTS

The iterative process of measuring on-site work generates a large amount of information, which is used by involved parties to determine project objectives and plan necessary action items. Use of devices such as PocketPC *(Cox et al. 2002)* to collect daily progress information is one of the traditional methods of performing progress monitoring. The collected data is recorded on a daily basis, and processed to include relevant information. Finally, the information is uploaded to project management software, and the project status is updated *(Del Pico 2013; Vick and Brilakis 2016)*. It can be inferred that the process of using such handheld devices for manually recording as-built information is labor intensive and the recorded information is prone to errors.

In an effort to overcome the disadvantages associated with the traditional methods of collecting as-built data from construction sites, several technologies have been tested and adopted for recording information. These technologies have been used either exclusively, or integrated with other technologies to collect as-built data. Examples of such technologies include using RFID (Radio-frequency identification) *(Chin et al. 2008)*, RFID and GPS (Global Positioning System) *(Ergen et al. 2007)*, barcode and GIS (Geographical Information Systems) *(Cheng and Chen 2002)*, lidar *(Turkan et al. 2012; Zhang and Arditi 2013; Kim et al. 2013; Tuttas et al. 2014; Tuttas et al. 2015; Son et al. 2017)* and photogrammetry *(Golparvar-Fard et al. 2009; Dimitrov and Golparvar-fard 2014)*. Several studies reported that using RFID and GPS technologies for progress monitoring have a common drawback that significant human effort is required for analyzing and processing the data *(Golparvar-Fard et al. 2009; Son et al. 2017).*

A number of studies have concluded that lidar and photogrammetry technologies can help automate construction progress monitoring. For example, Golparvar-Fard et al. *(2009)* developed a four dimensional augmented reality model (D^4-AR) to help project managers identify

discrepancies between as-built and as-planned progress. The as-built data is collected and recorded in the form of photographs on a daily basis. The structure-from-motion (SfM) technique was then used to extract geometric information by reconstructing a 3D model from photographs acquired at various angles. The information included the collected photographs that are used to generate progress information, which is then integrated into the 4D BIM. Although the approach is robust to occlusions, it is not sensitive to the variations in the density of 3D data. The economic benefits of using cameras for communication with project stakeholders for large construction projects are discussed in *(Bohn and Teizer 2009)*. This study highlighted the benefits and drawbacks of using high-resolution cameras for tracking the progress of construction projects. The researchers quantified the amount of savings generated as a result of using cameras for various tasks during construction.

Bosché et al. *(2009)* proposed an object recognition method based on a-priori knowledge that correctly identified the status of 88% of steel columns in lidar data. A progress tracking system, based on the object recognition algorithm proposed in *(Bosché 2010)*, was proposed by Turkan et al. *(2012)*. The system integrated schedule information into 3D BIM and used it together with lidar data to monitor the progress of construction. Based on the methodology described in the paper, a comparison is made between the number of elements recognized in the lidar data and the number of components that are expected to be complete within a given time period. In this way, the calculated progress rate information is continually uploaded in the 4D BIM, until the end of the project. One drawback associated with this method is that a user is required to manually register the BIM and the point clouds within the same coordinate system at the beginning, prior to processing the data. It also requires linking the 3D BIM and the project schedule manually, which is somewhat time consuming. However, it has to be done only once at the beginning of the project. The researchers concluded that an effective scan planning methodology to supplement the proposed progress tracking system could be a step further toward achieving a fully automated system.

Zhang and Arditi *(2013)* developed a progress tracking system that calculates the percentage of work completed by comparing the collected point cloud data with a 3D model. Since the tests were carried out in a laboratory, the factors which could interfere with the quality of the collected scan were not considered. Furthermore, the test specimens used for the study had simple geometries, making it easier for the object detection algorithm to recognize an object. The components of a building structure often have more complex geometric shapes than those tested in this study. Thus, the validity of the system for detecting such elements remains to be tested. Although insignificant human intervention is required in the object identification and progress measurement phase, this system also requires manual input during the registration process. A progress tracking method developed by Kim et al. *(2013)* is based on a repetitive process of comparing the collected as-built lidar data with a BIM model that regularly updates the status of construction activities. The method is built upon the assumption that delay may not be encountered and that there are no discrepancies between the actual and planned schedule. However, in reality, construction projects often experience unwanted delays. The automatic schedule updating system proposed by Son et al. *(2017)* automatically updates schedules in Microsoft Project; however, the registration of as-built and as-planned data is performed manually in the study. A review of related techniques for automatically reconstructing BIM representing as-built conditions using lidar data is presented in *(Tang et al. 2010)* and the validity of some of these approaches was tested in this project.

El-Omari and Moselhi (2009) utilized RFID, lidar, and photogrammetry technologies to develop a progress monitoring and control system. One major drawback of this approach is the process of identifying and pairing common points between the collected lidar data and photographs, which is quite laborious. Table 2.1 shows the performance of different technologies used for construction project progress measurements (*Kopsida et al. 2015, NCHRP 2013, Vick and Brilakis 2016*).

Table 2.1: Comparison of Performance of Various Technologies for Construction Progress Measurements (Kopsida et al. 2015, NCHRP 2013, Vick and Brilakis 2016)

	Technology			
	RFID	**GPS**	**Laser Scanners**	**Photogrammetry**
Accuracy (Good, Mediocre, Poor)	Mediocre	Good	Good	Mediocre
Data analysis	Partially Automated	Partially Automated	Fully Automated	Fully Automated
Time for setup	Installation > 1 hr	Setup < 1 hr	Setup < 1 hr	Minimal set-up time
Mobility of equipment	Handheld	Handheld	Heavy Equipment	Handheld
Project Location	Indoors and Outdoors	Outdoors	Indoors and Outdoors	Indoors and Outdoors

As described above, several studies have focused on using lidar for monitoring progress of building construction projects. Nevertheless, *no studies were found that have used lidar technology, notably mobile lidar technology, for monitoring progress of transportation construction projects.*

2.2 TECHNOLOGIES USED IN TRACKING TRANSPORTATION CONSTRUCTION PROJECTS

Satellite-based navigation systems such as GPS, Unmanned Aircraft systems (UAS), and RFID sensors have been used to assess productivity and to keep track of critical resources in projects that require earthwork calculations *(Navon and Shpatnitsky 2005; Pradhananga and Teizer 2013; Siebert and Teizer 2014; Vasenev et al. 2014)*. Jaselskis et al. *(2003)* demonstrated the use of lidar data collected using a terrestrial laser scanner for calculating and estimating the volume of rocks and soils. The researchers concluded that using lidar as the preferred surveying method is efficient and effective compared to traditional surveying methods. In transportation construction projects, it is important to track on-going site activities and to ensure that they have not deviated from their planned schedule. Jeong et al. *(2015)* described how information from Daily Work Reports (DWR) can be used for acquiring daily updates and tracking the progress of transportation projects. The researchers integrated the information collected from adjacent days and obtained the information about completed activities.

Lidar is mainly used for surveying tasks in transportation projects. The guidelines for implementing mobile lidar technology have been provided in Olsen et al. *(2013) and* (learnmobilelidar.com). Schneider *(2013)* states that lidar is a popular choice among state DOTs.

However, its high initial implementation cost is identified as being one of the biggest barriers to widespread adoption of this technology. Yen et al. *(2014)* investigated the economic implictions of adopting mobile lidar technology. Using data from programs implemented by the Washington State Department of Transportation (WSDOT) and California Department of Transportation (Caltrans), the researchers concluded that a majority portion of the initial implementation costs were attributable to equipment costs, personnel salary, transportation costs, and the costs associated with the collection and processing of data. The primary benefits of using this technology were identified as increased productivity and significant reductions in manual labor and carbon dioxide (CO_2) emissions from the fleet. The researchers demonstrated how $6.1 million in savings were achieved over three data-collection cycles, covering a period of 6 years. The study pointed out that the savings increased with the completion of each cycle as opposed to having a constant amount of savings for each cycle. The large savings in cost arising from the utilization of mobile lidar technology can be attributed to the concept of "collect once, use many". Data collected once can be stored for future use and used for multiple applications. Table 2.2 shows the comparison of properties of lidar datasets obtained using different lidar systems (Leica, NCHRP 2013, Trimble, Velodyne, Vick and Brilakis 2016).

Table 2.2: Comparison of Performance of Different Lidar Platforms for Construction Progress Tracking (Leica, NCHRP 2013, Trimble, Velodyne, Vick and Brilakis 2016)

	Lidar Platforms			
	Aerial Lidar (manned)	**Aerial Lidar (unmanned)**	**Mobile Lidar**	**Terrestrial Lidar**
3D Position Accuracy	20 – 30 cm	± 3 cm at 100 m	± 2 cm at 100-200 m	± 3 mm at 50 m - ±6 mm at 100 m
Resolution	5 – 15 pts/m^2	50-100 pts/m^2	100-1000 pts/m^2	100 – 1000 pts/m^2
Cost	$1,000,000	$50,000 - $500,000	$300,000 - $1,000,000	$16,000 - $200,000
Data Pre-processing	Raw data requires several steps of processing	Raw data requires several steps of processing	Raw data requires several steps of processing	Raw data can be used after minimal processing
Equipment Setup	Mobile	Mobile	Mobile	Stationary

Utilizing lidar for measuring work progress overcomes inaccuracies in data and saves time, compared to using manual methods such as DWR. The application of lidar and 4D modelling for progress tracking is yet to be evaluated for transportation projects.

2.3 CURRENT CIM/BIM FOR INFRASTRUCTURE PRACTICES – USE OF ND DESIGN MODELS AND LIDAR IN THE TRANSPORTATION INDUSTRY

Along with the increasing complexity of construction projects, the demands for improving construction workflows and the quality of work performed have also steadily increased over the years. Several research studies have investigated how technology can be leveraged for supporting construction management tasks. Advanced digital tools and technologies are

replacing traditional methods of acquiring as-built data, thus improving project delivery *(Guo et al. 2017)*. A smooth transition from 2D paper-based project delivery to a 3D digital data-based delivery method can be achieved using such tools and technologies.

Through an initiative called Every Day Counts (EDC) undertaken by the FHWA, new transportation technologies, innovations and processes are promoted every two years. The initiative involves participation of representatives from state transportation departments, local governments, tribes and private industry. The participants identify and implement innovations to reduce the duration of the project delivery process, foster environmental sustainability and improve traffic operations and safety *(Federal Highway Administration 2010)*. EDC-2 initiative focused on promoting the use of 3D design models in the transportation construction industry, while EDC-3 initiative focused on the use of 4D and 5D design models as well as the use of lidar to create accurate as-built record drawings for transportation projects.

The fundamentals of Civil Integrated Management (CIM) comprises the implementation of a wide array of advanced technologies, tools, and practices for collecting, organizing, and managing data pertaining to transportation infrastructure projects *(Adam et al. 2015) (O'Brien et al. 2016)*. The adoption and implementation of such advanced technologies and tools in transportation projects is similar to the use of BIM in building construction projects *(Guo et al. 2014)*. According to Sankaran et al. *(2016)*, the rate of adoption of CIM technologies in the transportation industry increased by 180% from 2009 through 2012. State transportation agencies have used CIM tools in transportation projects for advanced 3D visualization, and for creating existing and proposed ground Digital Terrain Models (DTMs) *(Sankaran et al. 2018)*. The study shows that adopting the Public-Private-Partnership (PPP) model for project delivery promotes better integration of CIM tools and technologies in the project workflow. The adoption of 3D modeling technologies by state DOTs has also been steadily increasing. Based on a study presented by FHWA *(FWHA 2013)*, digital 3D modelling workflows have replaced 2D design workflows in 23 DOTs. Based on the study, FHWA also reported that seven DOTs relied entirely on 2D drawings and fifteen DOTs are making the transition towards 3D modeling based workflows. Furthermore, FHWA lists the most commonly used software by DOTs for improving overall project performance including Microstation, InRoads, Geopak, and Autodesk Civil 3D. Nevertheless, for the state DOTs, although generated from 3D models, 2D plans are still the governing documents, and included as part of the legal binding contract documents. Typically, if requested, state DOTs provide their 3D model to the contractor, however in several states, the contractor must sign a liability form when receiving the model that limits the DOT from liability associated with use of the 3D model, but is not required on ODOT projects. Singh (2008) provides the ODOT vision for implementing new technologies and tools in their projects and processes, while particularly focusing on engineering automation. One of the technologies included in Singh (2008) is digital signatures. The Oregon State Board of Examiners for Engineering and Land Surveying (OSBEELS) approved to accept digital signatures in 2008, which has enabled 3D design models that are stamped and approved, to be included in the contract documents.

CIM assist with modelling, data management, and monitoring of construction projects and are used to improve overall project performance. Sankaran et al. *(2016)* states that bridging the gap between traditional project delivery and digital project delivery is possible through the use of new technologies for supporting project management tasks. The circulation of information

among involved parties and the coordination between the members of the parties are greatly enhanced through the adoption of CIM technologies.

2.3.1 Current CIM/BIM for Infrastructure Practices by Oregon Department of Transportation (ODOT)

Oregon is one of the leading states in the adoption of Intelligent Construction Systems and Technologies (ICST). The Oregon Department of Transportation (ODOT) has adopted and implemented numerous CIM tools and technologies including 3D design models, lidar, drones, and tablet computers for improving the overall performance of their projects. In 2014, ODOT held an event titled "Design to Paver" and presented the latest technological advancements in the transportation construction industry. Some of the advancements showcased include automatic stakeless grading, which integrated satellite positioning and digital 3D models to improve grading productivity. Intelligent compactors, that use GPS and infrared technology for enabling pass counts and temperature mapping, were also demonstrated in the field. Using such compactors ensured better accuracy and quality of the finished work. The utilization of UAVs for visualizing jobsite conditions and for surveying and mapping observation with the help of acquired imagery was also demonstrated. Several key concepts of engineering automation were also presented during the two-day event. Currently, ODOT develops 3D design models (typically delivered in XML format) for all their highway projects requiring earthwork, and provides these models to their contractors *(ODOT, 2012).* In return, contractors provide the 3D model they use on their machines back to ODOT for review. However, 3D design models are not a mandatory part of the construction contracts, and contractors are not required to use them. The current ODOT bridge design process follows a 2D workflow; however, there are plans to move toward 3D design in the near future. ODOT uses various lidar technologies, including mobile and terrestrial lidar, very effectively for the design phase of their projects as well as for inventory purposes.

ODOT has contributed toward pushing the frontiers of scientific research in many areas by funding several civil, construction, and geomatics engineering research projects. Some of the projects include using drones for a bridge inspection project (SPR787), lidar to determine International Roughness Index (IRI) (SPR744) of pavements and examining distractions during driving caused by drones. Several of these projects have used lidar data for project development, management of assets, evaluation of pavements, and monitoring of landslides. In one of these projects, Terrestrial Laser Scanning (TLS) point clouds were used for the quantification of erosion rates and surface deformation *(OTREC-RR-11-23) (Olsen et al. 2012)*. Additional on-going projects (SPR 740, 786, and 808) utilize lidar for landslide inventorying and hazard mapping at a landscape scale *(Leshchinsky et al. 2018)*. Additionally, a recently completed project funded by ODOT assessed the appearance and retro-reflectivity of pavement markings using mobile lidar data, and developed a road marking extraction tool (SPR 799) *(Olsen et al. 2018)*. As mentioned above, one of the CIM technologies used by ODOT is drones, i.e., unmanned aerial vehicles. ODOT uses drones to collect as-built or condition data from the areas or structures that are hard to reach or not safe to access. Tablet computers are also used for construction inspection purposes by ODOT. The utilization of advanced technologies such as lidar and 3D design models in this study is well-aligned with the key concepts presented by ODOT for the future. The concepts were presented as the guidelines for directing ODOT's future

engineering automation efforts, which ultimately enable the integration of technologies and tools in routine construction tasks *(Singh 2008)*.

2.4 DISCUSSION

Adoption of reliable and accurate technologies by DOTs to support project management tasks has created new challenges. One of the primary challenges is identifying appropriate technologies and tools that could help address the needs of a project. BIM software that is available for building projects is more mature and advanced than currently available software for BIM for Infrastructure. Current practices in GIS provide support for asset management, but do not encompass the necessary tools required to support progress monitoring tasks. Although both lidar and 3D design models are being used in multiple applications by DOTs, their potential for monitoring construction of transportation projects warrants more exploration, as was also discussed at ODOT's design to paver workshop. Using 3D design models in conjunction with lidar data can provide numerous benefits to DOT infrastructure projects, such as savings in cost and time, as discussed in Section 2.2. Therefore, this study aims to explore how progress monitoring tasks can be significantly improved through the use of these technologies in transportation projects.

Studies have shown that lidar technology combined with 4D Design models has great potential in improving construction progress monitoring *(Turkan et al. 2012; Zhang and Arditi 2013; Kim et al. 2013; Braun et al. 2015; Tuttas et al. 2014; Son et al. 2017)*. The utilization of these technologies has been well illustrated in the building construction industry, but requires evaluation and testing in the transportation construction industry. The frameworks developed for reporting the progress in horizontal construction projects report progress of a construction element in terms of binary values (0 for not detected and 1 for detected). However, it would be beneficial to have the progress information about some construction elements in percentage form. Thus, the following research question was developed for the study:

> *What steps should be taken to design a progress tracking framework that reports the progress of incremental work in horizontal construction projects, in terms of percentage of completion (what percent of a bridge element is complete), as opposed to binary output (element detected or not detected)?*

3.0 EXPERIMENTAL DESIGN

3.1 CASE STUDY

The selection of a suitable bridge construction project was important for this study. To be suitable for data collection, the project had to meet the following requirements.

- The project must be preferably in the initial stages of construction, so that the construction of each bridge element can be captured.
- The data collection cycles should be tentatively based on the provided construction schedule. This is important to make sure that the as-built data for each bridge element is captured. If a particular data collection cycle is too long, the construction of some bridge elements may not be captured.

In this study, the Truax Creek Bridge Replacement project located in Albany, OR was selected for the case study. The project involved demolishing the existing bridge structure and building a new one. At the time the research team started collecting data from the site, the northbound lane had already been completed, but was not yet open to traffic. The traffic was operating on the southbound lane. The new bridge is approximately 108 feet in length and 42 feet in width. Figure 3.1 shows the construction site. The scans were collected from the construction site on a weekly or bi-weekly basis, depending on the work scheduled for a particular week. At the end of each scanning period, the progress was recorded in the captured scans. These results were compared with traditional tracking methods.

Figure 3.1: Study site, Truax Creek Bridge in Albany, OR. Left: Google maps showing the location of the bridge. Right: Photo showing the southbound lane near its completion date.

3.2 EQUIPMENT

Data was collected using a Topcon IP-S2 mobile lidar mapping system previously owned by ODOT (Figure 3.2). The system integrates Velodyne's HDL-64E S2.2 3D lidar scanner with an inertial measurement unit (IMU) and GNSS sensor for positioning. The acquired data, however, has a lower accuracy compared to that can be collected using ODOT's current Leica Pegasus 2 system. The lidar sensor on the IP-S2 consists of 64 individual lasers, and can collect up to 1.3 million points/second. The sensor delivers a 360° field of view perpendicular to its axis and a 26.8° field of view parallel to its axis. Topcon IP-S2 mobile lidar mapping system includes a ladybug camera system that can capture 360° panoramic or spherical images, which can be useful for interpretation of the point cloud data. However, it was not operational during most of the data collection cycles.

Figure 3.2: Transfer of the Topcon IP-S2 mobile lidar mapping system from ODOT to OSU through an interagency agreement

4.0 METHODOLOGY

4.1 DEVELOPMENT OF THE PROPOSED FRAMEWORK

The proposed framework uses 3D mobile lidar point clouds and 4D design models (3D design model + project schedule) to continuously track bridge construction progress. This process entails the registration of the as-built and as-designed data in the same coordinate system. The next step involves segmentation of the point cloud and object recognition where bridge elements are detected. Based on the object recognition results, the deviation between the planned and actual work are quantified. This framework is discussed in detail in the following sections of this chapter and is summarized in Figure 4.1 (grey and orange boxes denote input/output data and data processing respectively). Hardware issues posed some challenges during some of the data collection cycles. The results of the object recognition algorithm used were validated partly through visual inspection of the scans.

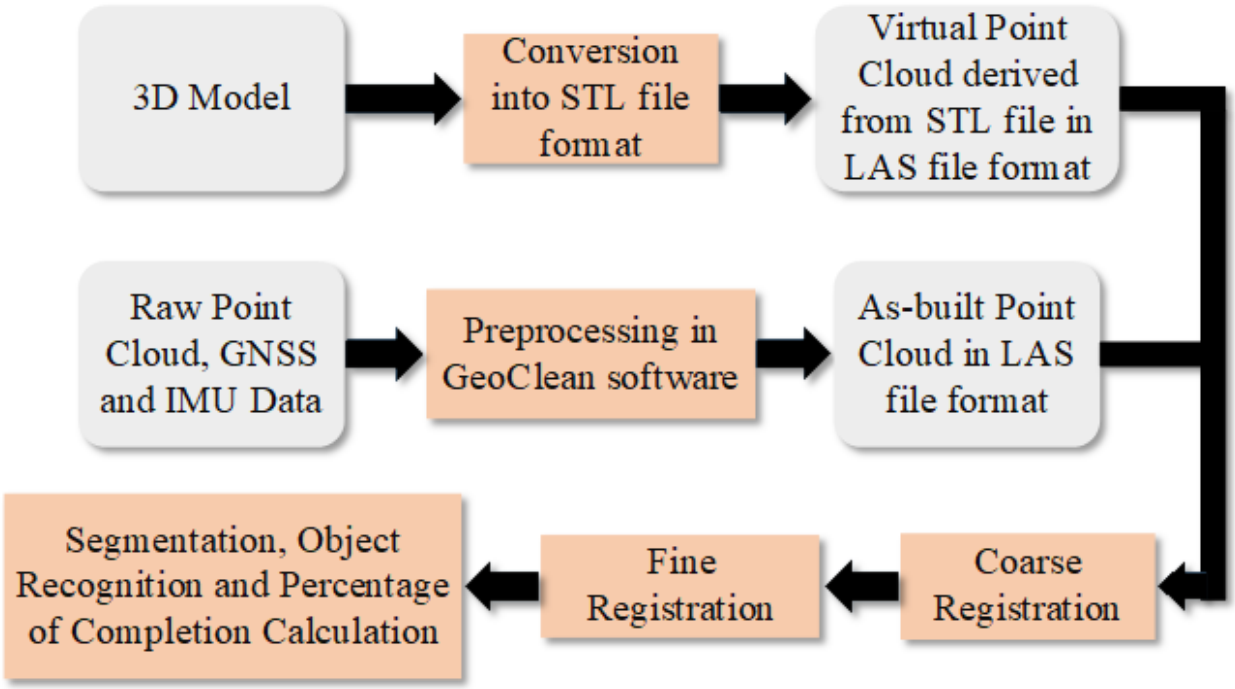

Figure 4.1: Overview of the proposed framework

4.1.1 Data Preprocessing

The raw mobile lidar data consists of ranges, angles, and timestamps that are referenced with respect to the origin of the scanner *(Williams et al. 2013)* as well as data from the GNSS and IMU sensors. After the data collection, GNSS (Global Navigation Satellite System) data from a reference station is downloaded from a nearby, permanent GNSS station to correct for

ionospheric disturbance and other systematic errors. Typically, these data are available in the form of Receiver Independent Exchange (RINEX) files from the Oregon Real Time Network maintained by ODOT, the National Geodetic Survey Continually Operating Reference Stations (CORs), or the Plate Boundary Observation (PBO) network maintained by UNAVCO. The raw data and the GNSS information are then imported into TOPCON Geoclean software, where the raw data is combined with GNSS and IMU data to generate 3D point clouds. If required, several point clouds from different passes can be collected and registered together into a single point cloud. They can also be combined with terrestrial laser scan data as needed. Color information is captured using a 360-degree ladybug camera and is mapped to each individual point in the point cloud *(Olsen et al. 2013).* The point cloud dataset can be saved in various file formats, some of which include LAS and E57 *(Olsen et al. 2013).*

4.1.2 Data Processing

After data preprocessing, the next step is to register the as-built data (3D lidar point cloud) and as-planned 4D model (3D design model (Figure 4.2) + project schedule) in the same coordinate system through coarse and fine registration steps. This process can be made more efficient by developing the 3D design model in the same coordinate system as the as-built point cloud. Once registered, an object recognition algorithm is implemented to detect the built elements in the point cloud. The discrepancies between the as-built and as-planned status of the project are identified by comparing the as-built point cloud data with the as-planned 4D model.

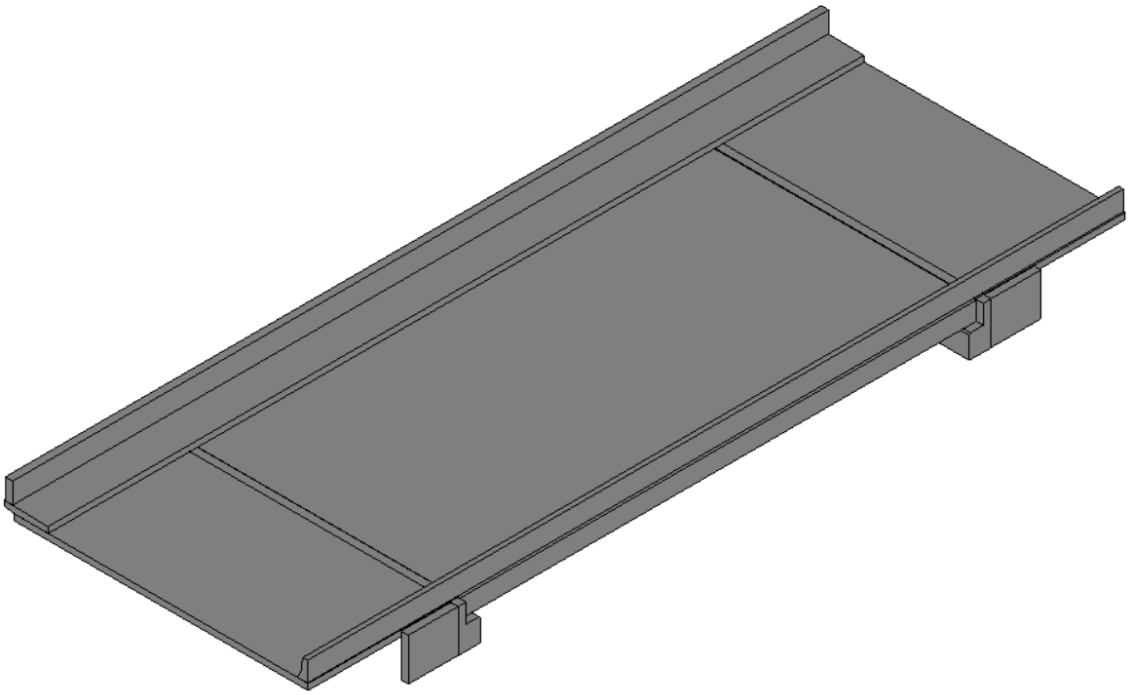

Figure 4.2: 3D model of Truax Creek Bridge, developed from the 2D design drawings

The 3D as-designed model needs to be converted into a triangulated mesh (STereoLithography (STL)) format before running the object recognition algorithm. This enables extracting as-designed points from the 3D model. These points are then manually matched to the

corresponding points in the 3D point cloud. The manual selection of points in the 3D model and point cloud data enables a quicker process of matching because elements that are similar in geometry can be identified and matched without errors, as compared to using an algorithm for matching the corresponding points *(Son et al., 2017)*. Furthermore, manually aligning the relevant portion of the point cloud with the 3D model overcomes the problem of occlusions *(Turkan et al., 2012)*. After manually aligning the point cloud and the 3D model, the registration is completed by fine-tuning the alignment using an Iterative Closest Point (ICP) algorithm *(Besl and McKay, 1992)*. For a particular scan date, based on the alignment between the 3D design model and the 3D point cloud, the object recognition algorithm that was developed in *(Turkan et al., 2012)* was adopted and modified for this project and used to segment a region of the point cloud in order to identify the objects in the 3D design model corresponding to that region.

4.1.2.1 Coarse and Fine Registration

After converting the 3D design model into STL file format, a virtual point cloud is generated by extracting the vertices of each of the triangulated faces present in the STL file. During both the coarse and fine registration steps, the as-built point cloud is fixed and the virtual point cloud is moving. The coarse registration process was completed by manually picking pairs of points between the as-built point cloud and the corresponding virtual point cloud. In Leica Cyclone, this process can be performed by first creating registration labels for several points in the models representing the corners of different elements. Those labels can be extracted into the as-built scans and re-used for facilitating the coarse registration process.

Upon the completion of the coarse registration process, the original as-built point cloud and the original virtual point cloud are finely registered using pairs of points in both point clouds. For a pair of points, one point belongs to the original virtual point cloud (query point), and the other point belongs to the original point cloud that is nearest to the query point. After this step, each of the points in the original virtual point cloud is matched with a corresponding point in the original as-built point cloud. When implementing this process, 7 cm was chosen as the threshold distance to account for the noise levels of the velodyne lidar system and construction errors. Figure 4.3 shows a slice of the alignment between the as-built (red, green and yellow colored points) and virtual point cloud (white colored points). From the distance between a pair of points in the as-built and virtual point clouds, it is evident that the scan data contains noise that is approximately 3-4 cm (1 sigma (σ)). Thus, 7 cm was chosen as the threshold to account both for noise in the as-built data and construction errors.

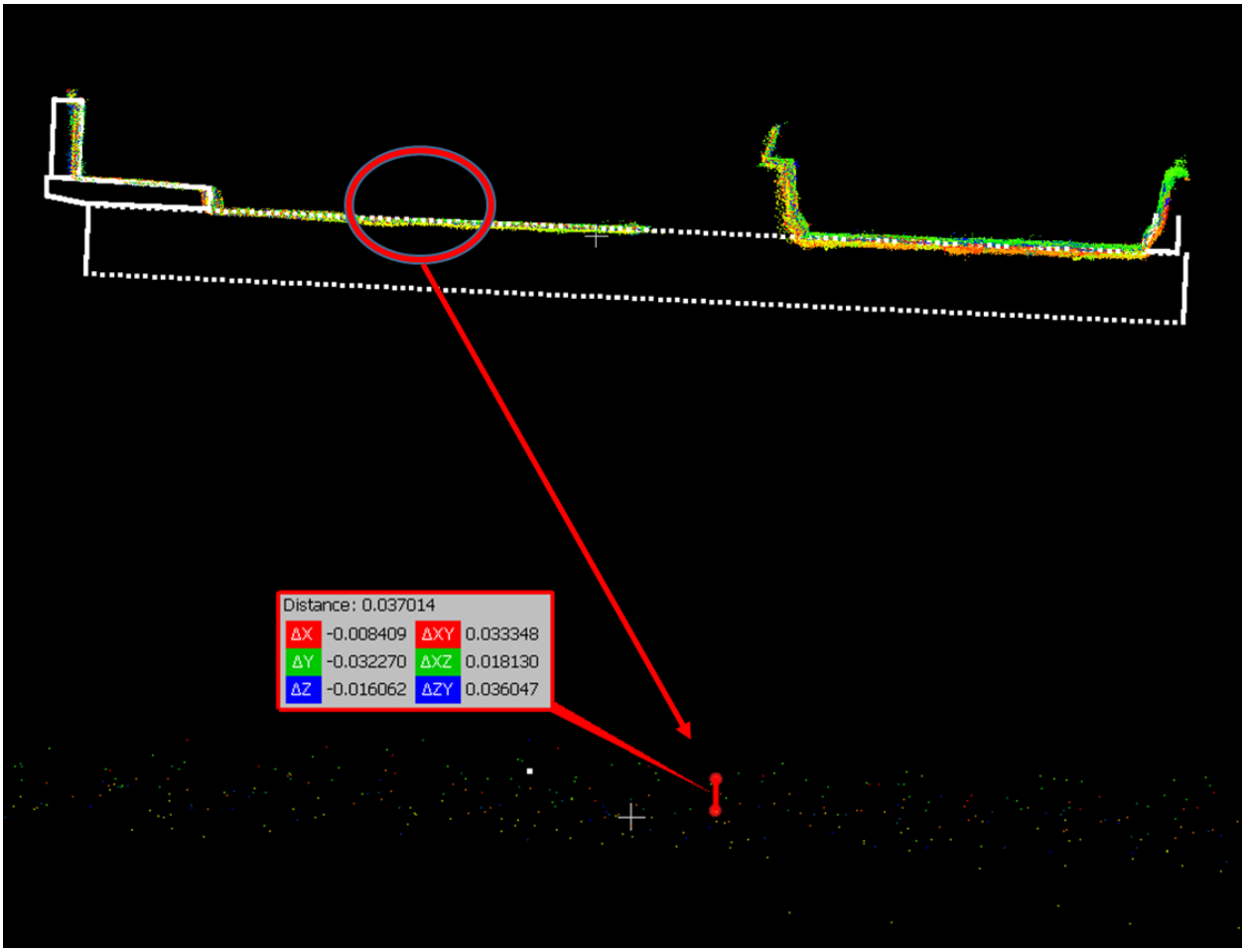

Figure 4.3: A section of the aligned as-built (red, green and yellow colored points) and virtual point clouds (white colored points) (scan date: August 22, 2018)

At the end of the coarse and fine registration steps, the coarsely registered as-built point cloud and the virtual point cloud are segmented to generate a subsampled version of both point clouds, containing an equal number of points. An equal number of points are obtained in both of the subsampled point clouds through a one-to-one matching process. After finding the matching pair of points between the as-built and virtual point clouds, an ICP algorithm is applied to fine-tune the coarse registration. The algorithm minimizes the Euclidean distance between a pair of points in an iterative manner. The iterations can be based on either a maximum threshold distance or a maximum number of iterations. In this study, since both of the subsampled point clouds have equal number of points, either can be chosen for facilitating the object recognition process. The subsampled virtual point cloud was chosen for further analysis, in our case, as detailed in section 4.1.2.2. At the end of coarse and fine registration steps, a composite transformation matrix combining the both transformation results was obtained and used in segmentation and object recognition steps.

Before implementing the segmentation and object recognition steps, STL files that were developed for each individual bridge element are used to generate corresponding virtual

point clouds for each of those elements. This step is important in order to keep track of individual bridge elements for a given date during the object recognition process. The coarse and fine registration processes are repeated for the virtual point clouds of individual bridge elements. This is achieved by applying the composite transformation matrix, obtained in the previous step, to each bridge element. This step helps facilitate the segmentation and object recognition process in the subsequent step. The fine registration step is summarized in Figure 4.4.

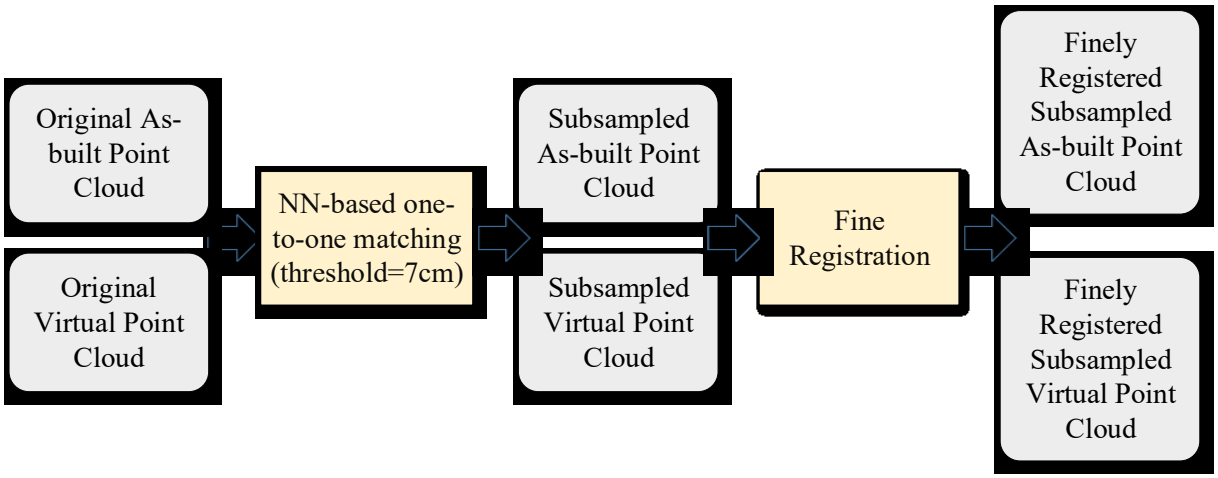

Figure 4.4: Overview of the fine registration step

4.1.2.2 Segmentation and Object Recognition

This step uses the subsampled virtual point cloud and finely registered virtual point cloud of each of the individual bridge elements obtained in the previous step. For a given scan date, an STL file of each bridge element is automatically aligned with the subsampled virtual point cloud corresponding to the entire bridge. The STL file of each bridge element carries the label of each bridge element, which is then passed onto the corresponding virtual point cloud of each bridge element. The STL file and the corresponding virtual point cloud were generated to help track individual bridge elements and their POC values for a given scan date. In the next step, the subsampled virtual point cloud is segmented automatically to extract the points corresponding to the bridge element in consideration. At the end of this step, a segmented subsampled virtual point cloud representing the as-built status of the corresponding bridge element for the given date is obtained. A case may arise where there is no overlapping region between subsampled virtual point cloud and finely registered virtual point cloud of an individual bridge element. This implies that the given element has either not been constructed yet, or has been constructed, but is obstructed from the scanner's view.

The segmentation process is facilitated by finding the nearest neighbor of each query point in the finely registered virtual point cloud of an individual bridge element, within the segmented subsampled virtual point cloud for a given scan date. The nearest neighbor search, similar to the previous step, is also carried out using the same predefined threshold, 7 cm. As explained in Section 4.1.2.1, at the end of the nearest neighbor

matching process in the registration step, the subsampled virtual point clouds were chosen instead of the subsampled as-built point clouds for further processing. Thus, the selection of the subsampled virtual point clouds is justified because the nearest neighbor matching process in this step can be performed between point clouds that are subset of the original virtual point cloud.

For a given bridge element, the one-to-one matching process between the segmented subsampled virtual point cloud and the finely registered virtual point cloud of the element yields a fragment of the segmented subsampled virtual point cloud that accurately represents the as-built status of that element for a given date. This fragment of the segmented subsampled virtual point cloud for a bridge element is an indicator that the bridge element is detected as constructed or under construction. The percentage of completion is calculated in the next step.

4.1.2.3 Percentage of Completion (POC)

After a particular bridge element is detected in the object recognition step, the status of completion of the element can be determined precisely by assigning it a percentage of completion (POC). For each virtual point cloud of an individual bridge element, the process of segmentation as described in Section 4.1.2.2 generates a point cloud that accurately represents the geometric as-built status for a given date. The alignment between obtained point cloud and the virtual point cloud of the individual element reveals the geometric faces of the element that overlap in the two scans. Depending on the bridge element type, the number of overlapping faces may vary. The part of the point cloud that represents the geometric face of the element with maximum number of overlapping points are chosen for the POC calculations. Convex hulls of the points covering that face is computed for both the virtual point cloud of the individual bridge element and the fragment of the segmented subsampled virtual point cloud for the element. The POC for an element *e* at a given date *d* is calculated by:

$$\mathbf{POC_{e,d}} = \frac{A}{A'} * \mathbf{100\ \%} \qquad \textbf{(4-1)}$$

Where:

> A represents the area of the convex hull of one of the common faces in the fragment of the segmented virtual point cloud of one as-built element. A' is the area of the convex hull of the same face in the virtual point cloud of the individual bridge element.

Let the dates of the scans be represented by $Date_1$, $Date_2$ and so on, where $Date_1$ represents the first day of scanning. If the construction of an element on a given date has not started yet, it is reflected in the output of the one-to-one matching process between the segmented subsampled virtual point cloud and the finely registered virtual point cloud of the element described in Section 4.1.2.2. An empty output resulting from this step indicates that the element was not detected in the as-built scan, whereas a non-empty

output signifies that an element was detected. Precedence relationships representing the dependencies of construction of one element on the other is developed to verify the POC calculated for all elements at a given scan date. The calculation of POC for all possible cases are summarized below:

1. If an element is recognized, $POC_{e,d}$ is the maximum value between the existing POC (if it exists) and the POC calculated using Equation (1) for that day. Note that the element may have an existing POC if one of its successors is more than 80% complete (using the information from the precedence relations). Majority of the bridge elements in this project were either 30%, 50% or 100% complete on different scan dates. In some cases, the elements that are fully constructed (100% complete) may be inaccurately reported to be 85% or 90% complete. In such cases, it would still be safe to assume that the predecessor of the bridge element is 100% complete if its successor is anywhere above 50% complete. As a conservative estimate, 80% was chosen. If the $POC_{e,2}$ is lower than the $POC_{e,1}$ for an element, $POC_{e,2}$ is set to the value of $POC_{e,1}$, and so on. This can be observed when the fully completed element is occluded from the scanner's view.

2. If an element is not recognized for reasons discussed above, $POC_{e,d}$ is set to the maximum value between zero and the existing POC (if it exists). Again, note that the element may have an existing POC if one of its successors is more than 80% complete.

3. Once the POCs for all elements for a particular scan date $Date_i$ are computed, the results are verified using the precedence relations. If the $POC_{e,d}$ reaches over 80% at a given date, the POCs for all other elements that are its predecessors during construction are set to 100%. This may also occur when a fully completed element is not visible to the scanner (occluded elements).

Figure 4.5 summarizes the steps described in Sections 4.1.2.2 and 4.1.2.3.

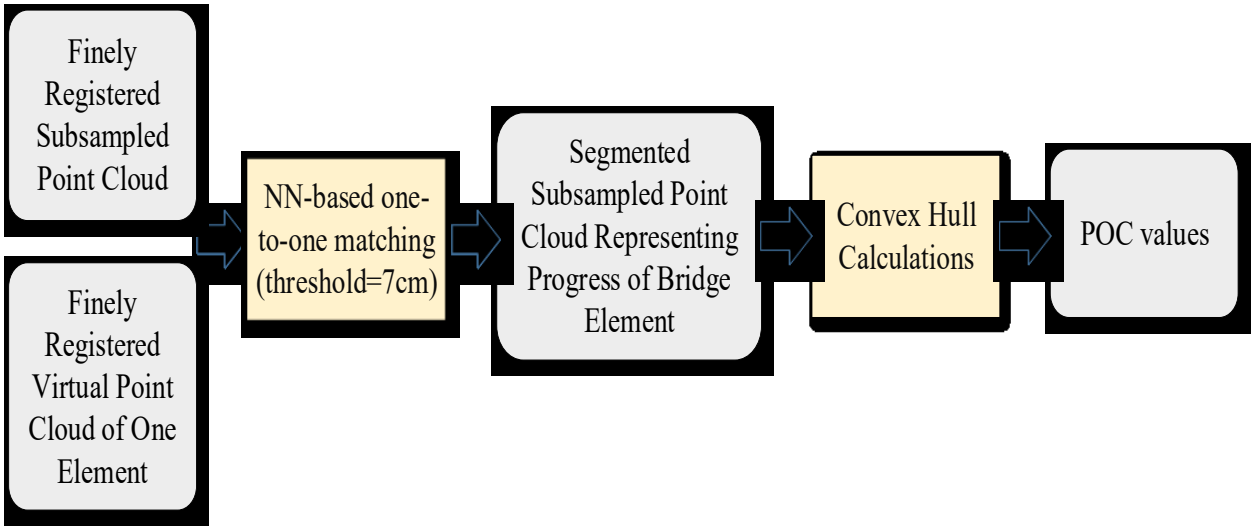

Figure 4.5: Overview of segmentation, object recognition and POC calculation steps

4.2 VALIDATION OF THE FRAMEWORK

The data collected from the Truax Creek Bridge construction project, as described in Section 3.1, was used for validating the framework. The as-built POC for the bridge project was calculated as described in Section 4.1.2.3. The as-planned POC was prepared manually by referring to the project schedule provided by ODOT (Figure 4.6).

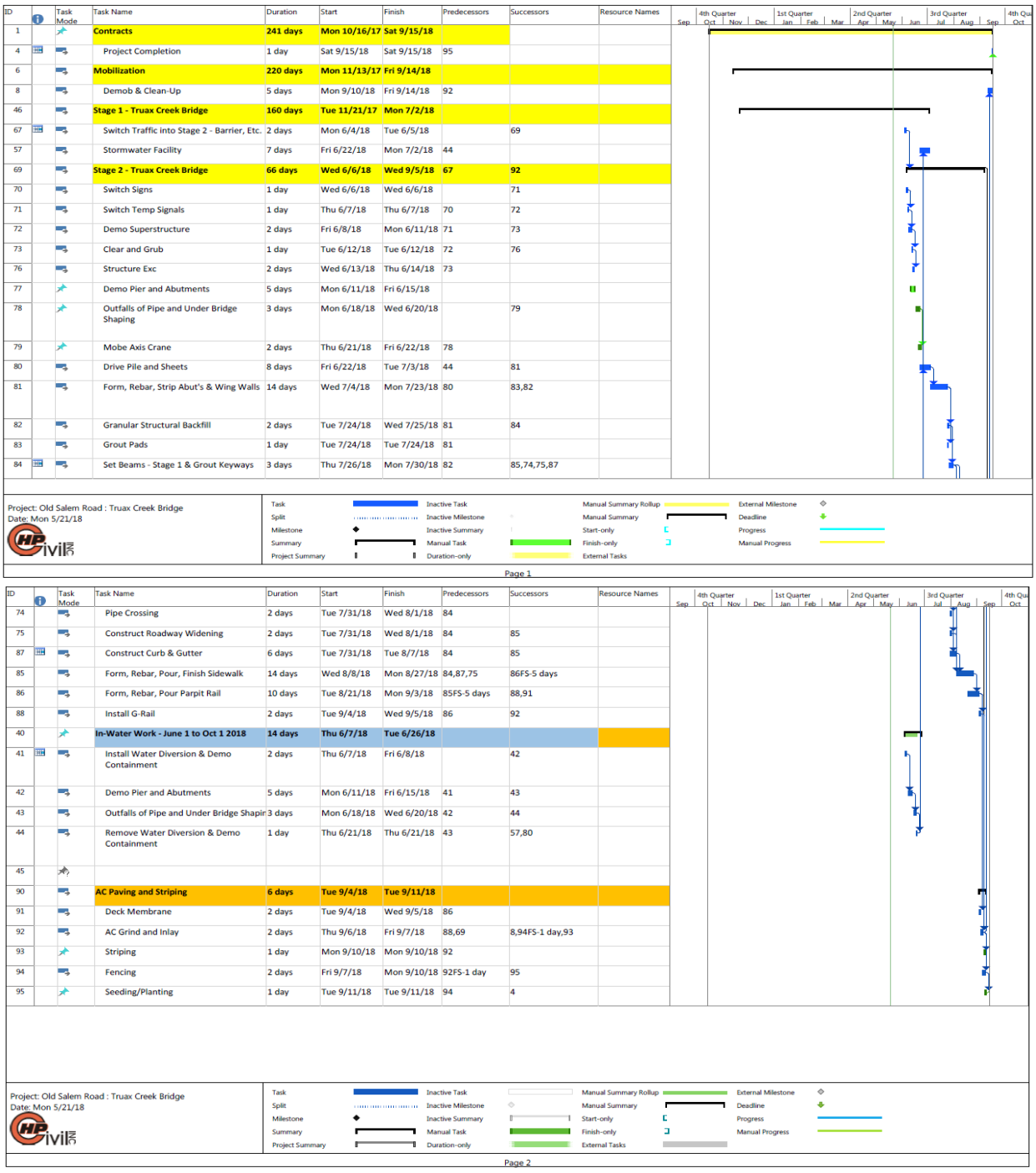

Figure 4.6: Schedule for the Truax Creek Bridge replacement project

5.0 RESULTS AND ANALYSIS

In this study, as-built data was collected using the mobile lidar system for the Truax Creek Bridge Replacement project located in Albany, OR. Two to three passes were made with the mobile lidar truck on each scan date. The information regarding the dates of data collection, number of passes and notes based on site observation are presented in Table 5.1.

Table 5.1: The Dates of Data Collection, Number of Passes during Each Data Collection Cycle and Notes Based on Site Observation

Scan date	Number of Passes	Notes
June 22, 2018	3	Northbound lane completed and traffic operating normally, earthwork in progress for the construction southbound lane Completed elements: North and South abutment, and two wing walls under the northbound lane complete but occluded from view
July 06, 2018	3	Earthwork on the southbound lane still in progress
July 13, 2018	2	Formwork for the abutments (north and south) and wing walls under the southbound lane was set up
July 24, 2018	3	Abutments and wing walls completed, deck placed on southbound lane
August 01, 2018	2	Deck and end panels complete
August 14, 2018	2	Sidewalk complete and formwork for parapet setup
August 22, 2018	2	Parapet still under construction
September 04, 2018	2	Parapet complete and railing installed
October 22, 2018	2	Asphalt Concrete Wearing Surface (ACWS) completed and construction finished

5.1 DEVELOPMENT OF THE PROPOSED FRAMEWORK

5.1.1 Data Processing

GNSS data, in the form of RINEX files, was downloaded from the National Geodetic Survey (NGS) Continuously Operating Reference Station (CORS) website. The files downloaded in .gz format were imported into TOPCON Geoclean software. The configuration of the base profile used for processing the GNSS data is shown in Table 5.2. A subset of the collected scans is shown in Figure 5.1.

Table 5.2: Base Profile Entry Configuration in Geoclean

Antenna Type	Dorne Margolin with chokerings, Model 70
Coordinate Type (IGS08 Epoch 2005)	ECEF
X [m]	-2498423.869
Y [m]	-38028020.840
Z [m]	4454737.819

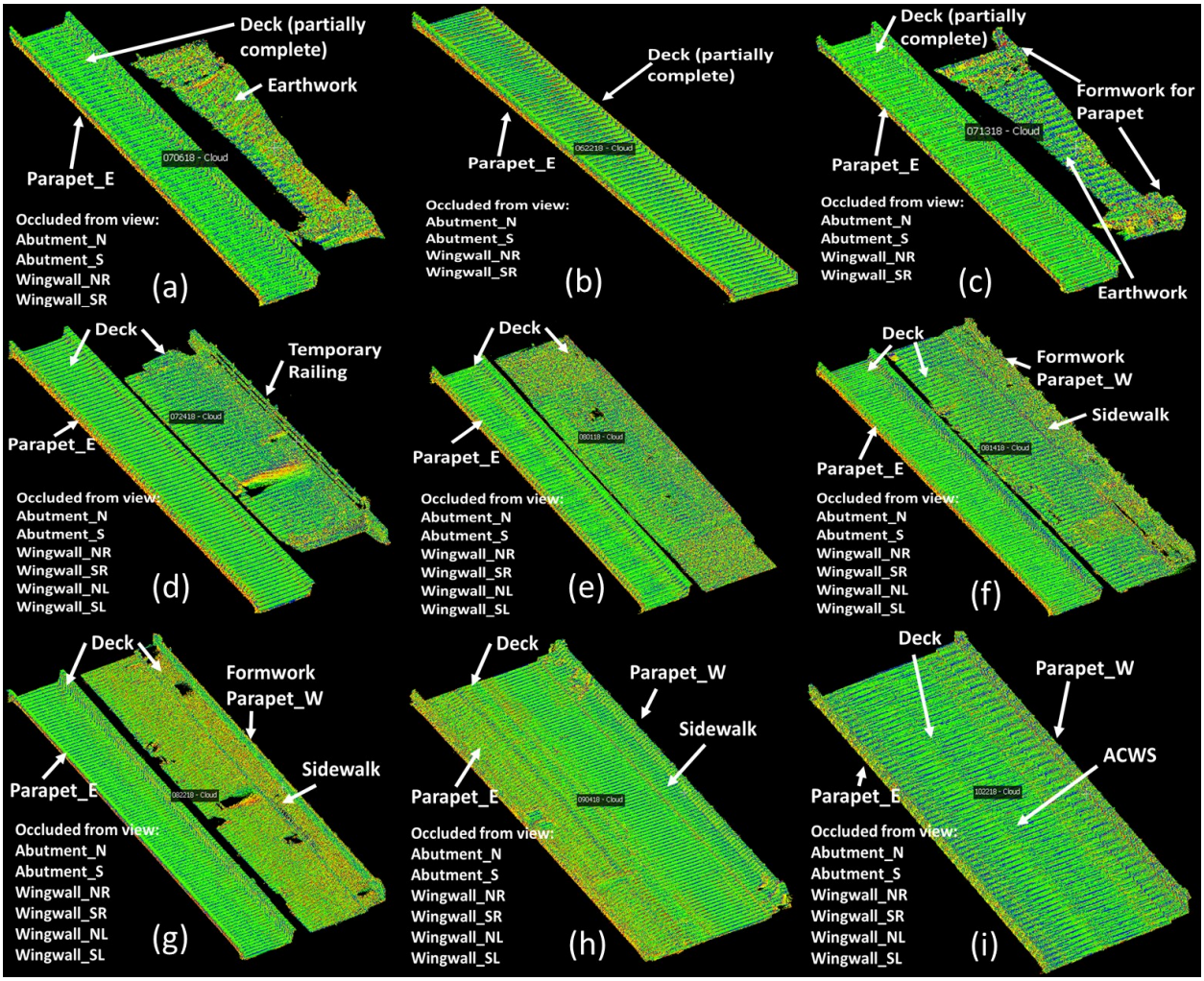

Figure 5.1: As-built point clouds collected on (a) June 22, 2018 (b) July 06, 2018 (c) July 13, 2018 (d) July 24, 2018 (e) August 08, 2018 (f) August 14, 2018 (g) August 22, 2018 (h) September 04, 2018 (i) October 22, 2018

5.1.2 Registration of As-built Data with As-planned Model

The as-built data coordinates were obtained from the lidar data collected using the mobile lidar unit, and matched with the coordinates extracted from the 3D as-designed model. The 3D design model of the Truax Creek Bridge was developed in Autodesk Revit software environment using

the 2D design drawings of the bridge, which were provided by ODOT. First, the model was exported to STL format using the STL exporter for Revit. Note that the .dgn files in Bentley Systems Microstation V8 could be exported from .dgn to .stl. However, the properties of the output STL file, including triangle count, could not be modified during the export. Thus, the exported STL file was imported into Gmsh, an open source software that allows further tessellation of the model, i.e. increase the triangle count. At the end of this process, another STL file of the model including 2,949,120 triangles was obtained. It is important to note that higher triangle count enables better one-to-one point matching process. The STL model is comprised of a tessellation of triangles that represent the geometric faces of the bridge elements in the 3D model. The .las files exported from the Geoclean software (original as-built point cloud), and the STL file of the bridge model (original virtual point cloud derived from it), are both imported into CloudCompare software for coarse registration. Figure 5.2 and Figure 5.4 show the original virtual point cloud derived from the STL file of the model, and the original as-built point cloud collected on 06/22/2017 respectively. Five points in the original as-built point cloud and the original virtual point cloud were selected for the coarse registration step. The output subsampled virtual point cloud and the subsampled as-built built cloud, obtained at the end of the one-to-one matching process, shown in Figure 5.3 and Figure 5.5, respectively.

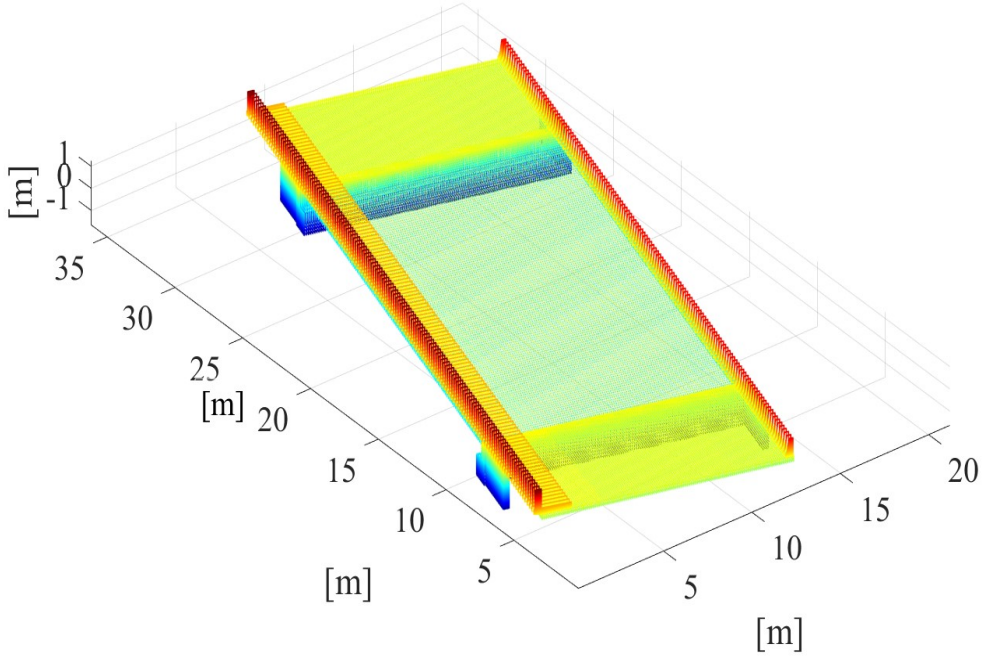

Figure 5.2: Original virtual point cloud derived from the STL model.

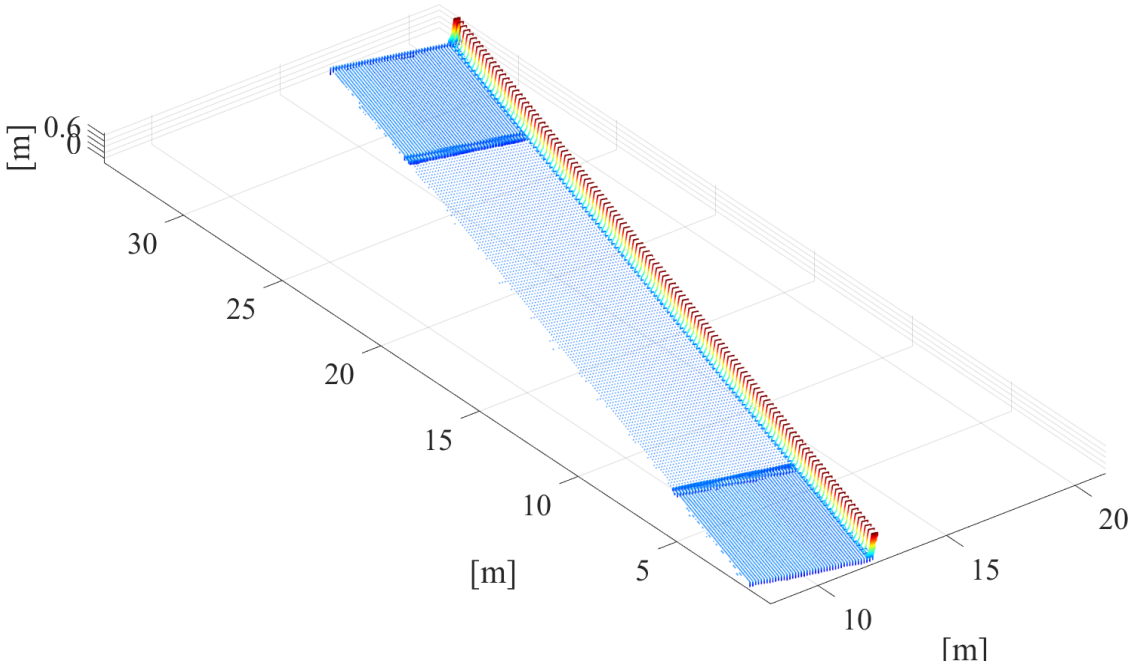

Figure 5.3: Subsampled version of the original virtual point cloud obtained from the STL model.

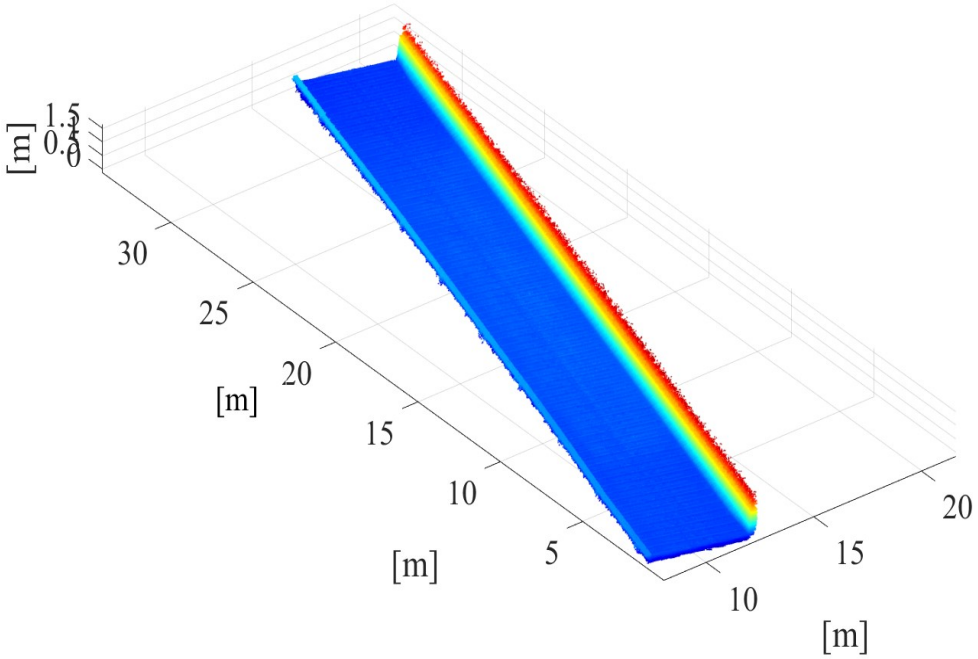

Figure 5.4: Original as-built point cloud scan collected on June 22, 2018.

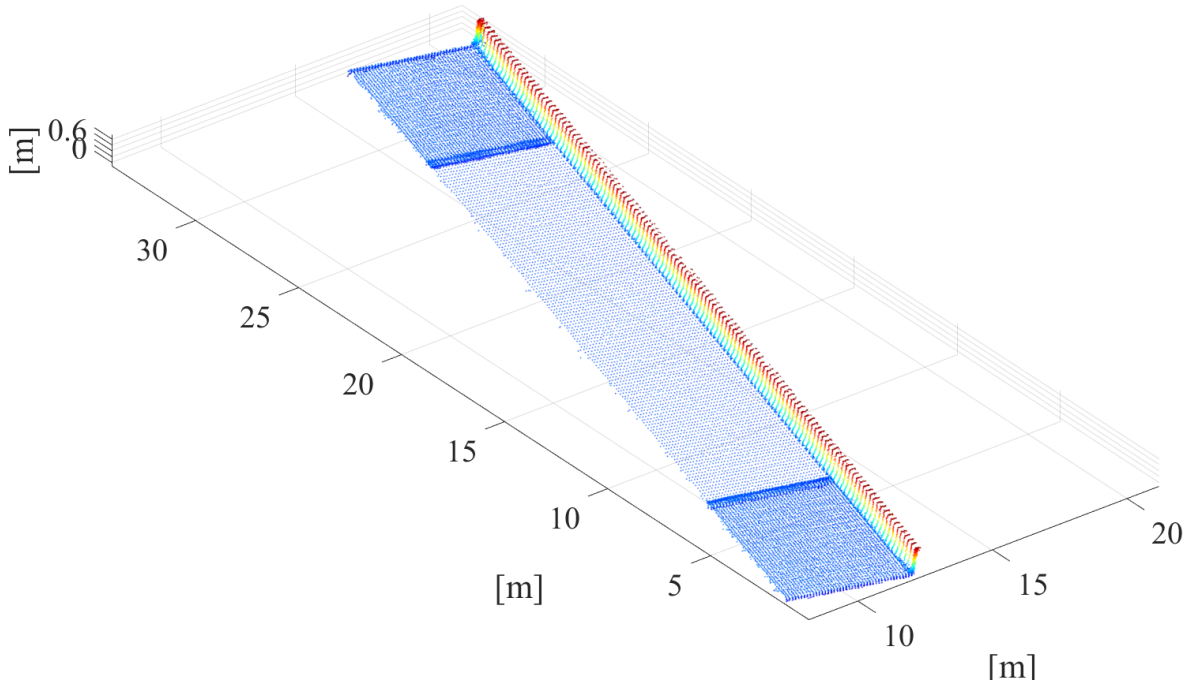

Figure 5.5: Subsampled version of the as-built point cloud collected on June 22, 2018.

After obtaining subsampled as-built and virtual point clouds containing equal number of points, the ICP algorithm was applied to fine-tune the registration. The fine registration process was carried out using a point-to-point based distance minimization metric, and the fine registration iteration is carried until the error between two consecutive iteration processes is less than 1*10^-6. The results of the registration process are shown in Table 5.33.

Table 5.3: Root Mean Square Errors (RMSE) Obtained at the end of Coarse and Fine Registration Steps for Each Scan

Scan Date	Number of Points in Original As-built Point Cloud	Number of Points after NN matching (before fine registration)	Fine registration RMSE [m]
6/22/2018	3,669,647	179,247	0.021
7/6/2018	3,983,640	257,160	0.028
7/13/2018	2,275,266	280,656	0.031
7/24/2018	5,151,269	350,009	0.030
8/1/2018	4,257,637	386,029	0.029
8/14/2018	6,082,413	351,194	0.030
8/22/2018	2,775,230	308,500	0.031
9/4/2018	6,327,087	375,488	0.024
10/22/2018	3,522,971	273,200	0.031

The consistent error values result from the 7 cm threshold, which was applied during the fine registration process.

5.1.3 Segmentation, Object Recognition and POC calculations

The segmentation process described in Section 4.1.2.2 is implemented for all elements at a given scan date and the object recognition results are obtained. The results are represented in the form of POC to accurately reflect the as-built status of the bridge elements. While performing segmentation between the segmented subsampled virtual point cloud and virtual point cloud of an element, one-to-one point matching performed by the nearest neighbor algorithm used a threshold of 7 cm. Figure 5.6 shows the result of the segmentation process applied to the bridge deck using the scan collected on June 22, 2018.

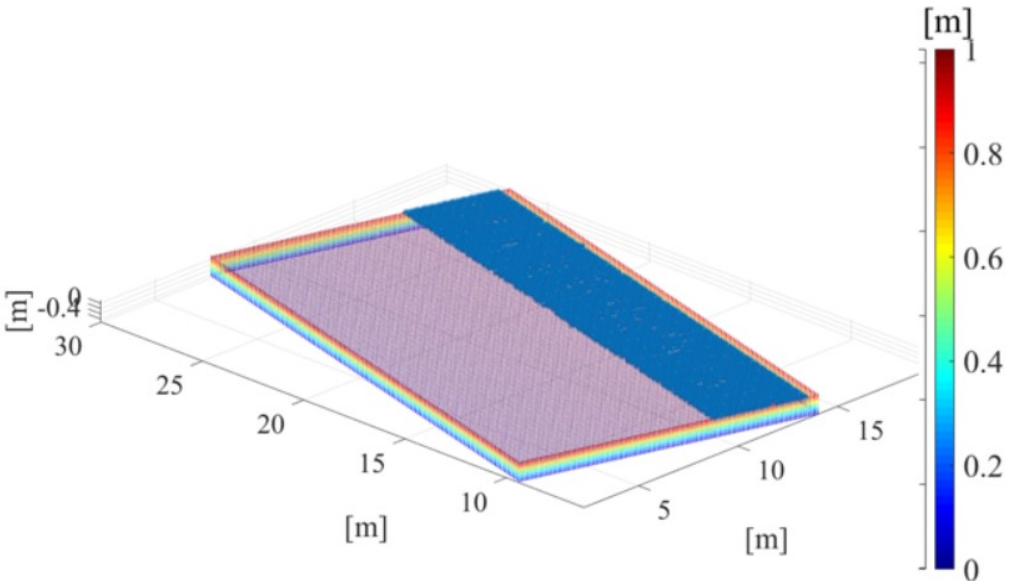

Figure 5.6: Fraction of the segmented subsampled virtual point cloud (shown in blue dots) obtained at the end of segmentation process between the subsampled virtual point cloud and the virtual point cloud of the bridge deck (scan date: June 22, 2018)

For our project, the use of a mobile laser scanner entailed that upper face of elements contained the maximum number of points that overlapped in the virtual point cloud of an individual bridge element and the fragment of the segmented subsampled virtual point cloud. The resulting convex hull for these point clouds are shown in Figure 5.7.

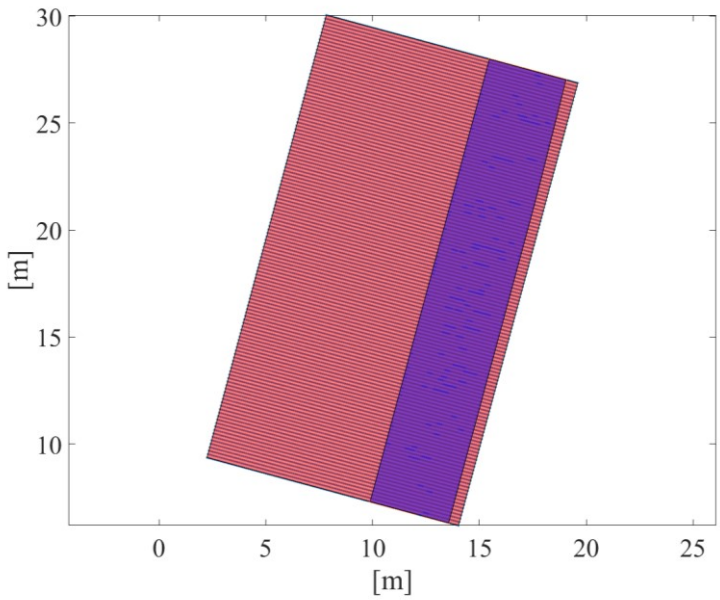

Figure 5.7: Convex hull for both point cloud datasets for the bridge deck (scan date: June 22, 2018)

The as-planned POC for all the scans collected were prepared manually by inspecting the project schedule obtained from the Engineer of Record. The purpose of preparing the as-planned POC is to help in validating the accuracy of the POC calculations. The as-planned and as-built POC for the project are shown in Table 5.4 and

Table 5.5 respectively.

Table 5.4: As-Planned POC (%)

Scheduled progress (%)	6/22	7/6	7/13	7/24	8/1	8/14	8/22	9/4	10/22
'Abutment_N'	30	30	50	100	100	100	100	100	100
'Abutment_S'	30	30	50	100	100	100	100	100	100
'BridgeEndPanel_N'	30	30	30	30	100	100	100	100	100
'BridgeEndPanel_S'	30	30	30	30	100	100	100	100	100
'Deck'	30	30	30	100	100	100	100	100	100
'Parapet_E'	100	100	100	100	100	100	100	100	100
'Parapet_W'	0	0	0	0	0	50	50	100	100
'Sidewalk'	0	0	0	0	0	100	100	100	100
'Wingwall_NL'	0	0	0	100	100	100	100	100	100
'Wingwall_NR'	100	100	100	100	100	100	100	100	100
'Wingwall_SL'	0	0	0	100	100	100	100	100	100
'Wingwall_SR'	100	100	100	100	100	100	100	100	100

Table 5.5: As-built POC (%)

Actual progress (%)	6/22	7/6	7/13	7/24	8/1	8/14	8/22	9/4	10/22
'Abutment_N'	31	35	35	100	100	100	100	100	100
'Abutment_S'	35	35	35	100	100	100	100	100	100
'BridgeEndPanel_N'	36	36	36	36	93	100	100	100	100
'BridgeEndPanel_S'	35	35	35	35	98	100	100	100	100
'Deck'	34	34	34	97	100	100	100	100	100
'Parapet_E'	99	100	100	100	100	100	100	100	100
'Parapet_W'	0	0	0	0	0	3	70	70	94
'Sidewalk'	0	0	0	1	5	100	100	100	100
'Wingwall_NL'	0	0	100	100	100	100	100	100	100
'Wingwall_NR'	100	100	100	100	100	100	100	100	100
'Wingwall_SL'	0	0	84	100	100	100	100	100	100
'Wingwall_SR'	100	100	100	100	100	100	100	100	100

5.2 VALIDATION

Table 5.6 shows the differences between as-planned and as-built POC values for all the bridge elements, i.e. the differences in corresponding POC values in Table 5.4 and

Table 5.5. The error values marked in yellow represent errors due to the limitations inherent in the convex hull algorithm that calculates overlapping area between the faces of the virtual and as-built point clouds, and the POC is defined as the ratio of these two. The planned POC may reflect an element to be 100% complete but the as-built POC may reflect it to be 96% complete. Practically, if such values are obtained, it can be interpreted as the slab being complete. The errors ranging from -6% to 6% in the yellow cells are the result of including or excluding a few as-built points belonging to these elements. This is likely to occur during the segmentation step since not all points (especially the ones on boundaries) are classified as belonging or not belonging to a particular element. Addition of a few points, depending on their location, can significantly impact the convex hull results, and consequently, the POC values. Visual inspection of the as-built scans belonging to these dates reveal that the corresponding values in Table 5.6 are reasonable.

Table 5.6: Differences in POC for all the bridge elements at the different scan dates (%)

Differences in POC (%)	6/22	7/6	7/13	7/24	8/1	8/14	8/22	9/4	10/22
'Abutment_N'	-1	-5	15	0	0	0	0	0	0
'Abutment_S'	-5	-5	15	0	0	0	0	0	0
'BridgeEndPanel_N'	-6	-6	-6	-6	7	0	0	0	0
'BridgeEndPanel_S'	-5	-5	-5	-5	2	0	0	0	0
'Deck'	-4	-4	-4	3	0	0	0	0	0
'Parapet_E'	2	0	0	0	0	0	0	0	0
'Parapet_W'	0	0	0	0	0	-3	-20	30	6
'Sidewalk'	0	0	0	-1	-5	0	0	0	0
'Wingwall_NL'	0	0	-10	0	0	0	0	0	0
'Wingwall_NR'	0	0	0	0	0	0	0	0	0
'Wingwall_SL'	0	0	6	0	0	0	0	0	0
'Wingwall_SR'	0	0	0	0	0	0	0	0	0

The values in the red cells indicate that the framework used in this study produced unacceptable results for some of the elements. For example, for the scan that was collected on July 13, 2018, the northbound abutment (*Abutment_N*) and the southbound abutment (*Abutment_S*) both show 15% error. Referring to the as-built scans, the formwork was set in place for both abutments on that date. The planned POC (Table 5.4) shows a value of 50%. This value was set to 50% from 35% on the previous scan date to indicate that installation of the formwork amounted to an additional increase in progress. Note that the right half (approximately 35%) of both abutments had been constructed by this date. Our framework calculates the POC based on the area of the convex hull spanned by the outermost points of the topmost face of the bridge element. The algorithm to calculate the convex hull is designed to discard points that are disconnected from the main cluster of points that accurately represent the as-built status of the element. In other words, as seen in Figure 5.8, the points encircled in blue are sparser compared to the points encircled in yellow. Thus, only the ones in yellow are considered in the convex hull calculations. Although the algorithm was specifically designed to handle cases, such as the one shown in Figure 5.9, it poses a limitation for certain cases.

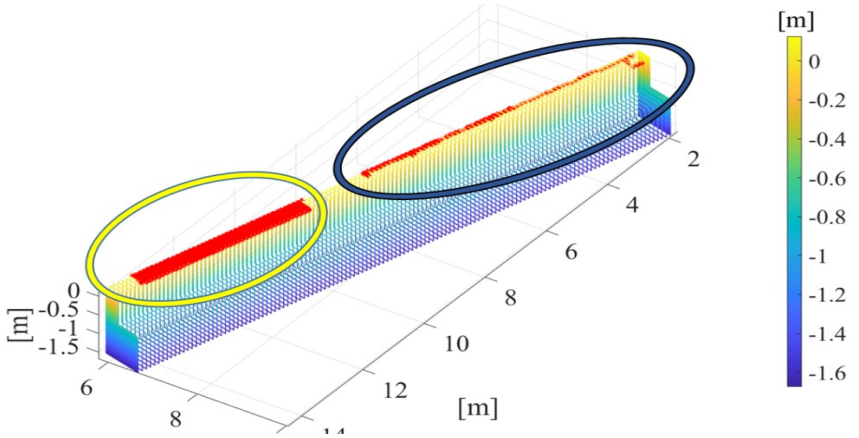

Figure 5.8: Virtual point cloud of southbound abutment with the point cloud representing the as-built status of the same element (red). The points encircled in yellow were included in convex hull calculations whereas the points encircled in blue are discarded.

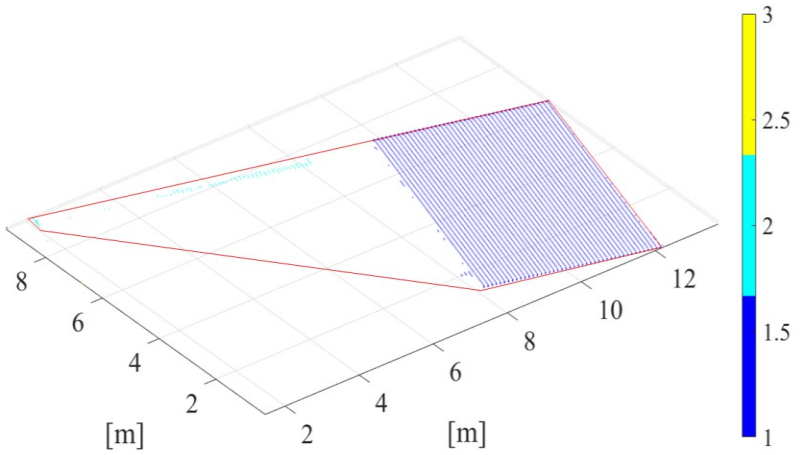

Figure 5.9: Outliers (in light blue) causing significant error in the convex hull calculations. The convex hull algorithm is designed to discard those points and keep the purple points.

Table 5.6 also shows erroneous values for the western parapet (*Parapet_W*) on scan dates August 22, 2018 and September 4, 2018. The corresponding values for this element in Table 5.4 shows that the western parapet is set to be 50% and 100% completed, respectively, on those dates. 50% was set for August 22, 2018 since most of the formwork and reinforcement bars had already been set up on that day. On scan date September 4, 2018, the parapet was complete. Figure 5.10 illustrates that the convex hull calculations did not account for the surface correctly. This is attributed to the fact that railings were not included in the 3D model and the top of the parapet was not modeled precisely to account for the placement of railings. Based on the provided schedule, it is assumed that the completion of the parapet signifies the completion of the railings placement. Similarly, this explanation applies to the error obtained (-10%) for the left northbound wingwall (*Wingwall_NL*) in the scan collected on July 13, 2018.

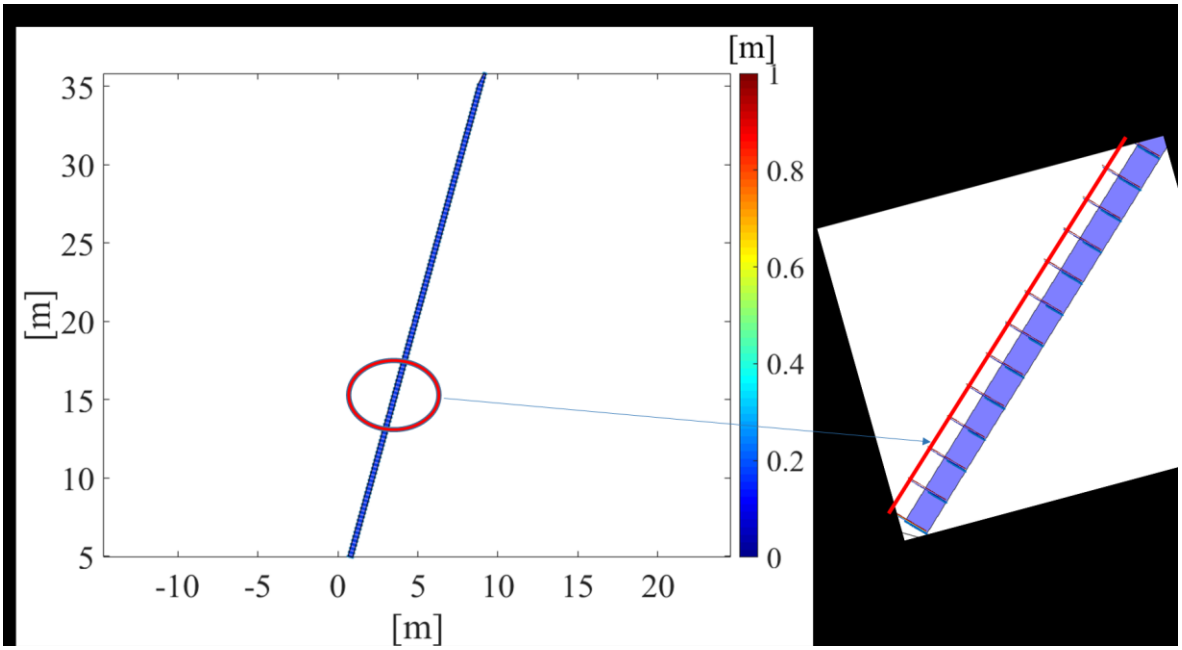

Figure 5.10: Western parapet convex hull (August 22, 2018). The right part represents an enlarged view of the convex hull. The red line on the enlarged section on the right side represents the extent of the area that should have been covered, and the blue region represents the area that was covered.

6.0 DISCUSSION AND LIMITATIONS

The performance of the proposed framework that was tested on the data collected from Truax Creek Bridge construction project was detailed in Section 5. Several factors may affect the quality of the progress tracking results, i.e. the POC values. For instance, the number of passes during the data collection can affect the density of the point cloud data obtained, which could impact the POC values. At the same time, the number of passes made during each data collection cycle has a direct impact on data collection time. The future research should investigate the number of passes required to obtain optimum results. Although the framework automatically computes the POC values, there are manual tasks which should be performed to support the automated processes described in the framework. The limitations of the proposed framework are detailed below.

Necessity of Manual Intervention

The presence of false positives directly impact the POC calculations. Thus, the initial process of manually removing false positives should be performed carefully. The removal process of false positives should ensure that points not belonging to the structure or part of the structure are completely removed. Figure 6.1 and Figure 6.2 illustrate this problem.

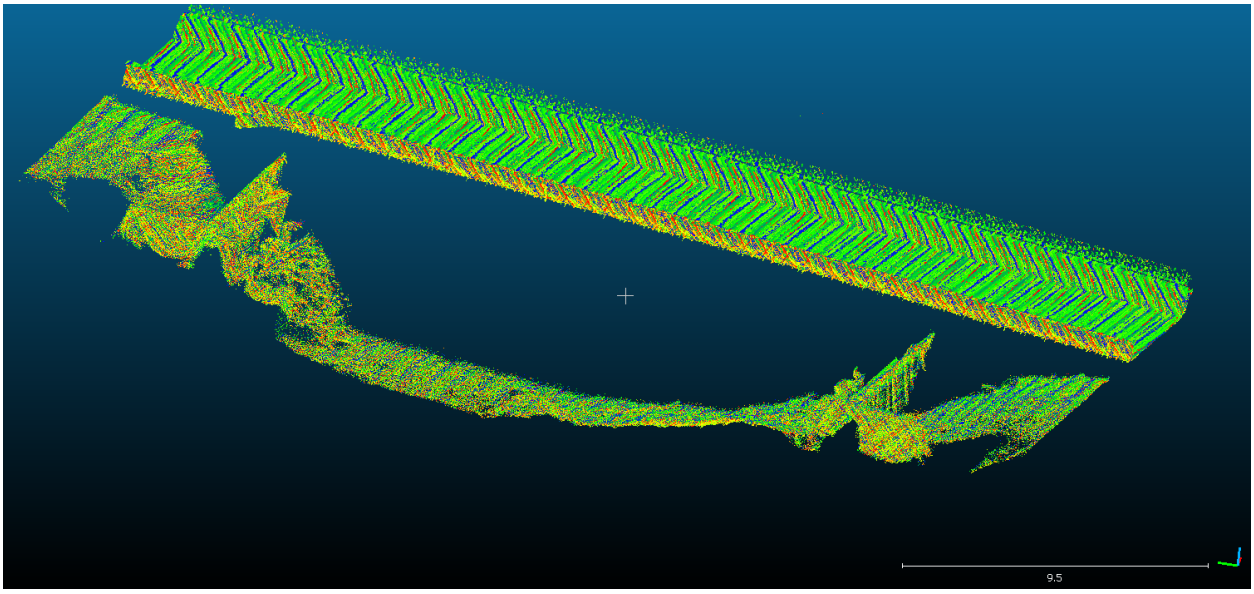

Figure 6.1: Scan collected on July, 13, 2018

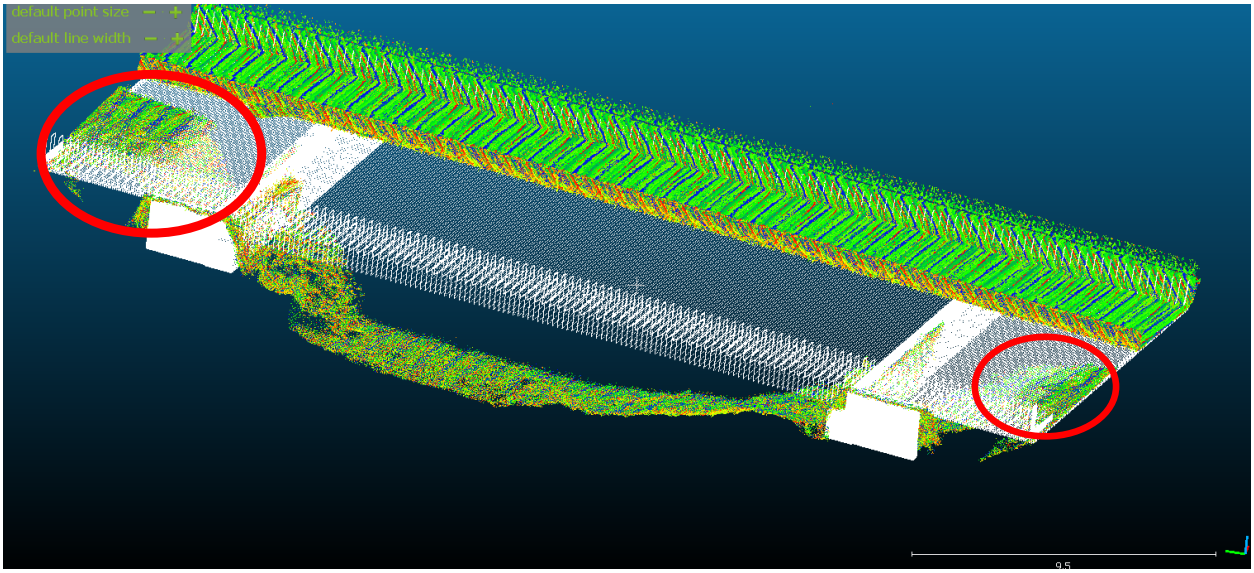

Figure 6.2: July, 13, 2018 scan overlapped with the finely registered original virtual point cloud. Regions of unwanted overlap bounded by red circles.

As shown in Figure 6.2, the part of the original virtual point cloud corresponding to the two bridge end panels have overlapped with the original as-built scans. During the object recognition phase, the progress of panels will be reported as "under construction", and will be assigned a percentage of completion, based on the percentage of overlap between the original virtual point cloud and the original as-built scans. Carefully cleaning the point cloud will result in better detection results.

Accuracy of the Mobile Mapping System

As shown in Figure 4.3, approximately one and a half inches noise was present in the as-built data. The presence of noise directly affected the selection of the threshold during the fine registration and segmentation steps described in Sections 4.1.2.1 and 4.1.2.2. Using a more accurate scanning system, such as the Pegasus system owned by ODOT can help overcome this limitation. Consequently, the threshold could be lowered by approximately one and a half inches, which should improve the accuracy of the POC calculations.

Processing time per epoch

Table 6.1 summarizes the approximate time taken for the manual and automated processes in the framework, including the software used for each step. Note that the orange color denotes processes that need to be performed only once. The blue color represents processes that have to be performed multiple times (refer to the comments column). Apart from manual processes that are required to be performed only once (highlighted in orange), the data processing time required for each epoch takes approximately 1 hour and 15 minutes. Please note that if a 3D project design at Level of Development (LOD) 300 is already available, it can be converted into STL format directly, which would lower the time required for manual processes to be performed manually at the beginning of the project (processes highlighted in orange) down to approximately 12 minutes. 3D models are becoming more and more common on ODOT projects;

hence, this time window would not need to be considered as time to utilize this workflow for progress monitoring.

Table 6.1: Time Taken for Manual Tasks for the Proposed Framework for the Case Study

Process	Software used	Time Taken	Comments
Data Collection			
Average time required for each data collection cycle	N/A	20 mins	Time includes 2-3 passes, depends on bridge length
Data Download and Upload to external hard drive (4 TB)	N/A	2 mins	For 15-20 GB file size, depends on data storage device used
Manual Processes			
*Development of 3D model (equivalent to BIM Level of Development 300 (LOD 300))	**Autodesk Revit	4-5 hours	Time includes studying 2D drawings
Creation of as-planned POC table	MS Excel	10 mins	
Generating STL files	Gmsh	2 mins	Per STL file
Manual Processes (per epoch)			
Point cloud pre-processing Geoclean	TOPCON Geoclean	20 - 30 mins	Per as-built point cloud
Point Cloud Cleaning (after preprocessing)	CloudCompare	15 mins	Per as-built point cloud
#Coarse Registration	CloudCompare	20 mins	Per set of as-built point cloud and virtual point cloud
Automated Processes			
Fine Registration (Approximate value, depends on size of point cloud)	MATLAB	15 mins	Per set of as-built point cloud and virtual point cloud
Segmentation, Object Recognition and POC calculations	MATLAB	5 secs	Per virtual point cloud of an object

Table Notes:
* 3D models are becoming more and more common on ODOT projects; hence this time source will likely already be invested in the design phase (with some updates in the construction phase as appropriate. Hence, it ordinarily will not be a significant source of time for progress monitoring.
** Instead of Autodesk Revit, Microstation by Bentley Systems or Autodesk Civil 3D can be used to develop 3D project models.
# The Coarse Registration step can be avoided by using a consistent coordinate system for the models and the mobile lidar data.

7.0 CONCLUSIONS

In this study, a progress tracking framework for transportation projects, bridge construction projects in particular, was developed and demonstrated. The framework combines information from 3D design models and construction schedule and lidar data to report project progress information. Using mobile lidar for as-built data collection provides significant benefits over manual methods for progress tracking by facilitating faster as-built data collection and accurately capturing 3D geometric information from construction sites.

The framework utilizes the project 3D model, at LOD 300 level, together with as-built data (in the form of lidar point clouds) to generate progress information. The 3D model data needs to be in STL file format, and lidar data needs to be in ASCII format (as .las files or .txt files). The software utilized for various processes required to implement the proposed framework are included in Table 6.1. Preparing a 3D model requires knowledge in conceptual massing or proficiency in using Revit or Microstation software. Familiarity with GeoClean software is necessary to import raw point cloud data, GNSS and IMU data together. Familiarity with various tools in CloudCompare software is required for manually cleaning the point cloud as well as for the coarse registration process. Therefore, implementing the framework presented in this report would require ODOT to have personnel with such skillsets and computing resources to process the lidar data.

The developed framework was evaluated using data collected from the Truax Creek bridge project, a small bridge construction project located in Albany, OR. The results of the case study showed that the developed framework enables tracking the completion of individual bridge elements accurately and efficiently. The process of obtaining progress results using the framework is mostly automated. The steps that require manual work include removing irrelevant sections in the preprocessed point clouds that overlap with bridge elements. The object detection relies upon the geometric alignment between the as-built point cloud and virtual point cloud. Hence, overlap between as-built data and irrelevant regions, such as earthwork material, may lead to misclassification. Furthermore, the manual processing time for each epoch is approximately 1 hour and 15 minutes for the case study. This time could be further reduced by continued development and refinement of algorithms to complete these manual processing tasks, which were beyond the scope of this project. Therefore, it can be concluded that the developed framework could be very beneficial when ODOT has multiple projects going on at the same time, which would require inspectors to travel between sites resulting in less frequent project status data collection. The semi-automated project progress tracking framework presented in this report would enable rapid collection of project as-built data, and determining project status in an efficient manner.

Future work should focus on implementing this framework on larger and more complex bridge construction projects that contain elements with complex geometrical shapes. The bridge used in this study was small and the project was almost 50% complete when the data collection had started. Furthermore, the entire framework utilizes only the x, y, and z coordinates of the collected scan. Future studies can be directed towards integrating RGB (Red-Green-Blue) values

and intensity values into the framework to help in material classification. Integrating RGB values can contribute toward accurate segmentation and object recognition results by correctly classifying points. The low quality data prevented performing this analysis for identifying the asphalt concrete wearing surface for the Truax Creek project. Using a high accuracy scanning system such as the Leica Pegasus: Two could help in road design layer classification. Additional parameters such as power spectral density could also be used to analyze the roughness of the profiles to distinguish one road design layer from another.

Finally, it is strongly recommended that the framework presented in this report be implemented on larger bridge construction projects, such as the Rose Quarter or the Columbia River Crossing where the return on investment (ROI) will likely be the highest compared with the implementation results presented in this report. Also, it is important to note that the digital documentation of construction projects could be very beneficial for legal purposes should issues on the project arise.

8.0 REFERENCES

Adam, J., Cawley, B., Petros, K., Brautigam, D., Burns, R., Burns, S., . . . Jahren, C. (2015). *Advances in Civil Integrated Management* (Scan 13-02, Publication No. 20-68A). Washington D.C.: National Cooperative Highway Research Program. Retrieved from onlinepubs.trb.org/onlinepubs/nchrp/docs/NCHRP20-68A_13-02.pdf.

American Road & Transportation Builders Association (2017). *U.S. Transportation Construction Market Forecast 2017*. ARTBA Transportation Development Foundation.

Arcuri, F. J. (2007). *A development of performance metrics for forecasting schedule slippage*. Blacksburg, Va.: University Libraries, Virginia Polytechnic Institute and State University.

Besl, P. J., McKay, N. D., Robotics - DL tentative 640679 1991-11-01|1991-11-07 Boston, MA, United States, Sensor Fusion IV: Control Paradigms and Data Structures 1611, & Robust Estimation of Shapes and Features 10. (April 30, 1992). Method for registration of 3-D shapes. *1611,* 586-606.

Bhargava, A., Anastasopoulos, P. C., Labi, S., Sinha, K. C., & Mannering, F. L. (November 01, 2010). Three-Stage Least-Squares Analysis of Time and Cost Overruns in Construction Contracts. *Journal of Construction Engineering and Management, 136,* 11, 1207-1218.

Bohn, J. S., & Teizer, J. (June 04, 2010). Benefits and barriers of construction project monitoring using high-resolution automated cameras. *Journal of Construction Engineering and Management, 136,* 6, 632-640.

Bosche, F. (January 01, 2010). Automated recognition of 3D CAD model objects in laser scans and calculation of as-built dimensions for dimensional compliance control in construction. *Advanced Engineering Informatics, 24,* 1, 107-118.

Bosche, F., Haas, C. T., & Akinci, B. (October 22, 2009). Automated recognition of 3D CAD objects in site laser scans for project 3D status visualization and performance control. *Journal of Computing in Civil Engineering, 23,* 6, 311-318.

Cantarelli, C. C., Flyvbjerg, B., van, W. B., & Molin, E. J. E. (January 01, 2010). Lock-in and its influence on the project performance of large-scale transportation infrastructure projects: investigating the way in which lock-in can emerge and affect cost overruns. *Environment and Planning. B, Planning & Design, 37,* 5, 792.

Cheng, M.-Y., & Chen, J.-C. (January 01, 2002). Integrating barcode and GIS for monitoring construction progress. *Automation in Construction, 11,* 1, 23-33.

Chin, S., Yoon, S., Choi, C., & Cho, C. (2008). RFID+4D CAD for Progress Management of Structural Steel Works in High-Rise Buildings. *Journal of Computing in Civil Engineering, 22*(2), 74-89. doi:doi:10.1061/(ASCE)0887-3801(2008)22:2(74)

Cox, S., Perdomo, J., & Thabet, W. (2002). Construction Field Data Inspection Using Pocket PC Technology. In *International Council for Research and Innovation in Building and Construction*(CIBw78). Blacksburg, VA: Virginia Tech.

Del Pico, W. J. (2013). *Project control: Integrating cost and schedule in construction*. Hoboken, NJ: RSMeans/John Wiley & Sons, Inc.

Dimitrov, A., & Golparvar-Fard, M. (January 01, 2014). Vision-based material recognition for automated monitoring of construction progress and generating building information modeling from unordered site image collections. *Advanced Engineering Informatics, 28,* 1, 37-49.

El-Omari, S., & Moselhi, O. (September 04, 2009). Data acquisition from construction sites for tracking purposes. *Engineering, Construction and Architectural Management, 16,* 5, 490-503.

El-Omari, S., & Moselhi, O. (October 01, 2011). Integrating automated data acquisition technologies for progress reporting of construction projects. *Automation in Construction, 20,* 6, 699-705.

Ergen, E., Akinci, B., & Sacks, R. (May 01, 2007). Tracking and locating components in a precast storage yard utilizing radio frequency identification technology and GPS. *Automation in Construction, 16,* 3, 354-367.

Economic Development Research Group,, & American Society of Civil Engineers,. (2016). *Failure to act: Closing the infrastructure investment gap for America's economic future*.

Federal Highway Administration (2010). *Every Day Counts Innovation Initiative: Prepared for the AASHTO Spring Business Meeting, May, 2010*. (Brochure). US Department of Transportation.

Flyvbjerg, B., Holm, M. K. S., & Buhl, S. L. (January 01, 2003). How common and how large are cost overruns in transport infrastructure projects?. *Transport Reviews, 231,* 71-88.

Geuzaine, C., & Remacle, J.-F. (September 10, 2009). Gmsh: A 3-D finite element mesh generator with built-in pre- and post-processing facilities. *International Journal for Numerical Methods in Engineering, 79,* 11, 1309-1331. Retrieved: February 18, 2019

Golparvar-Fard, M., S. Savarese, and F. Peña-Mora. (June 01, 2009). D4AR-A 4-dimensional augmented reality model for automating construction progress monitoring data collection, processing and communication. *Electronic Journal of Information Technology in Construction, 14,* 129-153.

Guidelines for the use of Mobile Lidar in Transportation. (n.d.). Retrieved January 30, 2018 from http://learnmobilelidar.com/

Guo, F., Turkan, Y., Jahren, C. T., & Jeong, H. D. (2014). Civil Information Modeling Adoption by Iowa and Missouri DOT. *Computing in Civil and Building Engineering (2014),* 463-471. doi:10.1061/9780784413616.058

Guo, F., Jahren, C. T., Turkan, Y., & Jeong, H. D. (2017). Civil Integrated Management: An Emerging Paradigm for Civil Infrastructure Project Delivery and Management. *Journal of Management in Engineering, 33*(2), 04016044. doi:10.1061/(asce)me.1943-5479.0000491

Jaselskis, E. J., Gao, Z., Welch, A., & O'Brien, D. (2003, August). Pilot study on laser scanning technology for transportation projects. In *Mid-Continent Transportation Research Symposium*.

Jeong, H. S., Gransberg, D. D., Shrestha, K. J., Mid America Transportation Center,, & United States. (2015). *Framework for advanced daily work report system: Final report about construction engineering*.

Kim, C., Son, H., & Kim, C. (May 01, 2013). Automated construction progress measurement using a 4D building information model and 3D data. *Automation in Construction, 31,* 75-82.

Kopsida, M., Brilakis, I.K., & Vela, P.A. (2015). A Review of Automated Construction Progress Monitoring and Inspection Methods.

Leica Geosystems. (n.d.). Retrieved January 30, 2018, from https://leica-geosystems.com/

Leshchinsky, B. A., Olsen, M. J., & Bunn, M. D. (2018). *Enhancing Landslide Inventorying, Lidar Hazard Assessment and Asset Management* (Publication No. FHWA-OR-RD-18-18). Salem, OR: Oregon Department of Transportation. Retrieved from https://www.oregon.gov/ODOT/TD/TP_RES /.

National Geodetic Survey, US Department of Commerce, Noaa, US Department of Commerce, & Noaa. (2009, August 17). National Geodetic Survey - CORS Homepage. Retrieved February 18, 2019, from https://www.ngs.noaa.gov/CORS/.

Navon, R., & Shpatnitsky, Y. (November 01, 2005). A model for automated monitoring of road construction. *Construction Management and Economics, 23,* 9, 941-951.

Nee, P. A. (1996). *ISO 9000 in construction*. New York, N.Y: J. Wiley and Sons.

O'Brien, W. J., National Academies of Sciences, Engineering, and Medicine (U.S.)., National Cooperative Highway Research Program,, American Association of State Highway and Transportation Officials,, & United States. (2016). *Civil Integrated Management (CIM) for Departments of Transportation: Volume 2*.

Olsen, M. J., Allan, J. C., & Priest, G. R. (January 01, 2012). Movement and Erosion Quantification of the Johnson Creek, Oregon, Landslide through 3D Laser Scanning. *Geotechnical Special Publication, 5,* 225, 3050-3059.

Olsen, M., V. Roe, G., Glennie, C., Persi, F., Reedy, M., Hurwitz, D., . . . Knodler, M. (2013). *Guidelines for the Use of Mobile LIDAR in Transportation Applications*.

Olsen, M. J., Raugust, J. D., Roe, G. V., National Research Council (U.S.)., National Cooperative Highway Research Program., American Association of State Highway and Transportation Officials., & United States. (2013). *Use of advanced geospatial data, tools, technologies, and information in Department of Transportation projects*. Washington, D.C: Transportation Research Board.

Olsen, M. J., Parrish, C. E., Che, E., Jung, J., & Greenwood, J. (2018). *Lidar for Maintenance of Pavement Reflective Markings and Retroreflective Signs: Vol. I Reflective Pavement Markings* (Publication No. FHWA-OR-RD-19-01). Salem, OR: Oregon Department of Transportation. Retrieved from https://www.oregon.gov/ODOT/Programs/Pages/Research.aspx.

Owolabi, J. D., L. M. Amusan, C. Olayinka Oloke, O. Olusanya, P. F. Tunji-Olayeni, O. Dele, N. J. Peter, and I. O. Omuh. (2014) Causes and effect of delay on project construction delivery time. *International journal of education and research*, *2,* 4, 197-208.

Pradhananga, N., & Teizer, J. (January 01, 2013). Automatic spatio-temporal analysis of construction site equipment operations using GPS data. *Automation in Construction, 29,* 107-122.

Sankaran, B., Nevett, G., Obrien, W. J., Goodrum, P. M., & Johnson, J. (2018). Civil Integrated Management: Empirical study of digital practices in highway project delivery and asset management. *Automation in Construction, 87*, 84-95. doi:10.1016/j.autcon.2017.12.006

Sankaran, B., O'Brien, W., Goodrum, P., Khwaja, N., Leite, F., & Johnson, J. (2016). Civil Integrated Management for Highway Infrastructure. *Transportation Research Record: Journal of the Transportation Research Board, 2573*, 10-17. doi:10.3141/2573-02

Schneider, C. (2013). *3D, 4D, and 5D Engineered Models for Construction*. US Department of Transportation. Retrieved from: https://www.fhwa.dot.gov/construction/pubs/hif13048.pdf.

Siebert, S., & Teizer, J. (May 01, 2014). Mobile 3D mapping for surveying earthwork projects using an Unmanned Aerial Vehicle (UAV) system. *Automation in Construction, 41,* 1-14.

Singh, R., & Oregon. (2008). *Engineering automation: Key concepts for a 25 year time horizon*. Salem, Or.: Oregon Dept. of Transportation, Highway Division.

Son, H., Kwon, C., & Y., Kim, C. (July 01, 2017). Automated Schedule Updates Using As-Built Data and a 4D Building Information Model. *Journal of Management in Engineering, 33,* 4.

Sumara, J. R., & Goodpasture, J. (January 01, 1996). Earned Value - The Next Generation: A Practical Application for Commercial Projects. *Proceedings- Project Management Institute,* 839-843.

Tang, P., Huber, D., Akinci, B., Lipman, R., & Lytle, A. (November 01, 2010). Automatic reconstruction of as-built building information models from laser-scanned point clouds: A review of related techniques. *Automation in Construction, 19,* 7, 829.

Trimble: Transforming the way the world works. (n.d.). Retrieved January 30, 2018, from https://www.trimble.com/

Turkan, Y., Bosche, F., Haas, C. T., & Haas, R. (March 01, 2012). Automated progress tracking using 4D schedule and 3D sensing technologies. *Automation in Construction, 22,* 414-421.

Turkan, Y., Bosché, F., Haas, C. T., & Haas, R. (April 01, 2013). Toward Automated Earned Value Tracking Using 3D Imaging Tools. *Journal of Construction Engineering and Management, 139,* 4, 423-433.

Tuttas, S., Braun, A., Borrmann, A., & Stilla, U. (August 11, 2014). Comparision of photogrammetric point clouds with BIM building elements for construction progress monitoring. *Isprs - International Archives of the Photogrammetry, Remote Sensing and Spatial Information Sciences, 3,* 341-345.

Tuttas, S., Stilla, U., Braun, A., & Borrmann, A. (February 01, 2017). Acquisition and consecutive registration of photogrammetric point clouds for construction progress monitoring using a 4D BIM. *Pfg - Journal of Photogrammetry, Remote Sensing and Geoinformation Science, 85,* 1, 3-15.

Vasenev, A., Pradhananga, N., Bijleveld, F. R., Ionita, D., Hartmann, T., Teizer, J., & Dorée, A. G. (October 01, 2014). An information fusion approach for filtering GNSS data sets collected during construction operations. *Advanced Engineering Informatics, 28,* 4, 297-310.

Velodyne Lidar. (n.d.). Retrieved January 30, 2018, from http://velodynelidar.com/

Vick, S. M., & Brilakis, I. (2016). A Review of Linear Transportation Construction Progress Monitoring Techniques. In *Proceedings of the 16th International Conference on Computing in Civil and Building Engineering* (pp. 1106-1113).

Williams, K., Olsen, M. J., Roe, G. V., & Glennie, C. (October 02, 2013). Synthesis of transportation applications of mobile LIDAR. *Remote Sensing, 5,* 9, 4652-4692.

Yen, K. S., Lasky, T. A., & Ravani, B. (December 01, 2014). Cost-Benefit Analysis of Mobile Terrestrial Laser Scanning Applications for Highway Infrastructure. *Journal of Infrastructure Systems, 20,* 4, 4014022.

Zhang, C., & Arditi, D. (December 01, 2013). Automated progress control using laser scanning technology. *Automation in Construction, 36,* 108-116.

APPENDIX: A

Matlab code

k-NN

```
function[New_A_c, New_B_c]=knn_dist(A_c,B_c,distance)
    %A_c and B_c are in double format


    P=pointCloud(A_c); %original lidar
    Q=pointCloud(B_c); %point cloud from STL
    tic;
    k=0;
    New_A_c={};
    New_B_c={};
    for j = 1:length(B_c)
        [i,dists] =
     findNearestNeighbors(P,Q.Location(j,:),1);
        if dists < distance
            New_A_c{1,1}(k+1,:)=A_c(i,:);
            New_B_c{1,1}(k+1,:)=Q.Location(j,:);
            k=k+1;
        end
    end
%     f=New_A_c;
%     g=New_B_c;
toc;
end
```

```
%     figure;

%     pcshow(pointCloud(New_A_c));

%     hold on

%     pcshow(pointCloud(New_B_c));

%     title('As-planned points matched with Point cloud')
```

Extract Dependencies from .txt file

```
function [depd]=dependencies()

    fid = fopen( 'C:\Users\purin\Box\OSU\papers\ODOT
     project\Truax Creek Files\Dependencies.txt' );

        cac = textscan( fid, '%s%s%s%s%s%s%s%s%s',
     'CollectOutput'  ...

                    ,   true, 'Delimiter', ','  );

        [~] = fclose( fid );

    % D=textscan('C:\Users\purin\Box\OSU\papers\ODOT
     project\Truax Creek Files\Dependencies.txt',',');

    Co=[cac{:}];

    cc=str2double(Co);

    depd=cc(:,2:end);
```

Fine Registration

```
%% read point cloud and stl file

function[New_a_pc_fReg,rmse,tform_comp,New_A_pc]=reg_ICP(A,
     a,b,thres)

%New_a_pc_fReg:segmented and registered
     (coarse+fine)virtual point cloud

%New_a_pc:segmented virtual point cloud
```

```
A_c=[A.x,A.y,A.z];



a_pc=[a.x,a.y,a.z];
b_pc=[b.x,b.y,b.z];

[regParams,~,~]=absor(b_pc',a_pc');
tform_coarse = affine3d(regParams.M');
figure;
%x=pctransform(pointCloud(b_pc),tform_coarse);
%     pcshow(x)
%     hold on
%     pcshow(pointCloud(a_pc))
%     hold on
%     pcshow(pointCloud(b_pc))



%% noise removal by finding nearest neighbours of each
 point in stl, in the point cloud
P=pointCloud(A_c); %as-built point cloud, fixed
Q=pointCloud(a_pc); %virtual point cloud, moving
%     figure;
pcshow(P);
title('Original As-Built Point Cloud');
xlabel('[m]')
```

```
ylabel('[m]')

zlabel('[m]')

a =
 annotation('textbox','EdgeColor','White','String','[m]'
 );

a.FontName = 'Times new Roman';

a.FontSize = 30;

set(gca, 'FontSize', 30, 'FontName','Times New Roman');

colormap(jet)


figure;

pcshow(Q);

title(' Virtual Point Cloud')

%[New_A_c,New_B_c]=knn_dist(A_c,B_c,distance)

tic;

k=0;

for j = 1:length(a_pc)

    [i,dists] =
 findNearestNeighbors(P,Q.Location(j,:),1);

    if dists < thres %accounting for noise and
 construction error

        New_A(k+1,:)=A_c(i,:); %part of original point
 cloud, fixed

        New_a_pc(k+1,:)=Q.Location(j,:);%part of
 virtual point cloud, moving

        k=k+1;

    end
```

```
end
figure;
pcshow(pointCloud(New_A));
title('Subsampled As-Built Point Cloud')
xlabel('[m]')
ylabel('[m]')
zlabel('[m]')

a.FontName = 'Times new Roman';
a.FontSize = 30;
set(gca, 'FontSize', 30, 'FontName','Times New Roman');
colormap(jet)
figure;
pcshow(pointCloud(New_a_pc));
title('Subsampled Virtual Point Cloud')
xlabel('[m]')
ylabel('[m]')
zlabel('[m]')

a.FontName = 'Times new Roman';
a.FontSize = 30;
set(gca, 'FontSize', 30, 'FontName','Times New Roman');
colormap(jet)
toc;
```

```
    tic;

    [tform_fine,New_a_pc_fReg,rmse] =
     pcregistericp(pointCloud(New_a_pc),pointCloud(New_A),'T
     olerance',[0.000001,0.000001]);

    %tform_fine: fine reg between original and virtual

    toc;

    T=tform_coarse.T*tform_fine.T;

    tform_comp=affine3d(T);

    %tform_comp is the coarse and fine reg combined

    %x_a=pctransform(pointCloud(b_pc),tform_comp);


%     pcshow(x_a)

%     hold on

%     pcshow(New_a_pc_fReg)


    %% plot reg resu;ts

%     figure(1)

%
     scatter3(New_a_pc(:,1),New_a_pc(:,2),New_a_pc(:,3),'.',
     'MarkerEdgeColor',[0 .25 .25])

%     hold on

%
     scatter3(A_c(:,1),A_c(:,2),A_c(:,3),'.','MarkerEdgeColo
     r',[0 .75 .75])

%     title(['Fine Registration RMSE = ' num2str(rmse) ])

end

%%
```

```
a=lasdata('C:\Users\purin\Box\OSU\papers\ODOT project\Truax
    Creek Files\3D model\CC_Binary_7_fr.las');

lidar_path=('C:\Users\purin\Box\OSU\papers\ODOT
    project\Truax Creek Files\Lidar data\');

out_folder='C:\Users\purin\Box\OSU\papers\ODOT
    project\Truax Creek Files\3D
    model\Elements\Fine_reg\Reconigtion\7 cm\as-built\';

Files_lidar=dir('C:\Users\purin\Box\OSU\papers\ODOT
    project\Truax Creek Files\Lidar data\*.las');

b=lasdata('C:\Users\purin\Box\OSU\papers\ODOT project\Truax
    Creek Files\3D model\Gmsh_Binary_7.las');



for j=1:length(Files_lidar)

    f = fullfile(lidar_path,Files_lidar(j).name);

    Y=lasdata(f);

    tic;

    [finereg_pc,rmse,tcomp,]=reg_ICP(Y,a,b,0.07);

    newFile =
     strcat(out_folder,Files_lidar(j).name,'.mat');

    save(newFile, 'as_built','rmse');

    toc;

end
```

```
function [surf_area]=area_convhll(B)

    row_idx=((max(B(:,3))-0.07)<B(:,3)).*(B(:,3)<
     max(B(:,3)));

    Row_idx=logical(row_idx);

    B_fil=B(Row_idx,:);

%     figure

%     pcshow(pointCloud(B_fil))

    %A and B pointclouds, type double

    g=pointCloud(B_fil);

            [labels,numClusters] = pcsegdist(g,1.5);

            pcshow(g.Location,labels)

            colormap(hsv(numClusters))

            title('Point Cloud Clusters')


       for i = 1:numClusters

            val(i) = sum(labels==i);

       end

       [m,i]=max(val);

           newer=B_fil(labels==i,:);

           figure

           pcshow(pointCloud(newer))


     vi = convhull(newer(:,1),newer(:,2));

     x1= newer(:,1);
```

```
    y1= newer(:,2);

    surf_area=polyarea(x1(vi),y1(vi));


    plot(x1,y1,'.')

    axis equal

    hold on

    fill ( x1(vi), y1(vi), 'b','facealpha', 0.5 );

    hold off

end









%

b=lasdata('C:\Users\purin\Box\OSU\papers\ODOT project\Truax
    Creek Files\3D model\Gmsh_Binary_7.las');

% %finereg_pc:segmented and registered (coarse+fine)virtual
    point cloud

% %finereg_fil_pc:segmented virtual point cloud (according
    to lidar)

% save('C:\Users\purin\Box\OSU\papers\ODOT project\Truax
    Creek Files\3D
    model\Elements\Fine_reg\Fine_reg_pc.mat',
    'finereg_pc','rmse');

%

out_folder='C:\Users\purin\Box\OSU\papers\ODOT
    project\Truax Creek Files\3D
    model\Elements\Fine_reg\Reconigtion';
```

```
Files_IFCBIM=dir('C:\Users\purin\Box\OSU\papers\ODOT
    project\Truax Creek Files\3D
    model\Elements\Fine_reg\*.las.mat');



recognition={};

dayy=1;

Files_lidar=dir('C:\Users\purin\Box\OSU\papers\ODOT
    project\Truax Creek Files\Lidar data\*.las');

%

for k=1:length(Files_IFCBIM)

    s=strsplit(Files_IFCBIM(k).name,'.');

    recognition{1,dayy}(k,1)=s(1);

end

tic;

% X=lasdata('C:\Users\purin\Box\OSU\papers\ODOT
    project\Truax Creek Files\Lidar data\082218.las');

Y=lasdata('C:\Users\purin\Box\OSU\papers\ODOT project\Truax
    Creek Files\Lidar data\090418.las');

a=lasdata('C:\Users\purin\Box\OSU\papers\ODOT project\Truax
    Creek Files\3D model\CC_Binary_7_fr.las');



% Z=lasdata('C:\Users\purin\Box\OSU\papers\ODOT
    project\Truax Creek Files\3D
    model\CC_Binary_7_fr.las');

% scatter3(X.x,X.y,X.z,'r','.')

% hold on

% scatter3(Y.x,Y.y,Y.z,'b','.')

% hold on
```

```
% scatter3(Z.x,Z.y,Z.z,'g','.')

lidar_path=('C:\Users\purin\Box\OSU\papers\ODOT
    project\Truax Creek Files\Lidar data\');


D=dependencies()

addpath('C:\Users\purin\Box\OSU\papers\ODOT project\Truax
    Creek Files\3D model\Elements\Fine_reg')

for j=1:length(Files_lidar)

%     f = fullfile(lidar_path,Files_lidar(j).name);

%     Y=lasdata(f);

%     tic;

%

%     [finereg_pc,finereg_fil_pc,rmse]=reg_ICP(Y,a,b,0.07);

%

%     newFile = strcat('C:\Users\purin\Box\OSU\papers\ODOT
    project\Truax Creek Files\3D
    model\Elements\Fine_reg\Reconigtion\',Files_lidar(j).na
    me,'.mat');

%     save(newFile, 'finereg_pc','rmse');

%     toc;

    for k=1:length(Files_IFCBIM)

        x=load(Files_IFCBIM(k).name);

        B=x.x_a.Location; %IFCBIM elements

        row_idx_B=((max(B(:,3))-0.07)<B(:,3)).*(B(:,3)<
    max(B(:,3)));

        Row_idx_B=logical(row_idx_B);

        B_fil=B(Row_idx_B,:);
```

```
   A=finereg_pc.Location;%segmented as planned point
cloud

   scatter3(A(:,1),A(:,2),A(:,3),'.')

   hold on

   pcshow(pointCloud(B_fil))

   [new_A,New_B]=knn_dist(A,B_fil,0.07); %find nearest
neighbours of the STL object points in the segmented
and registered (coarse+fine)virtual point cloud

   if size(new_A)~=0

       scatter3(new_A{1, 1}(:,1),new_A{1,
1}(:,2),new_A{1, 1}(:,3),'*','r')

       hold on

       pcshow(pointCloud(B))

       figure;

        title(' Overlap between the Segmented
Subsampled Virtual Point Cloud and the Virtual Point
Cloud of the Bridge Deck  ')

       xlabel('[m]')

       ylabel('[m]')

       zlabel('[m]')

       a =
annotation('textbox','EdgeColor','White','String','[m]'
);

       a.FontName = 'Times new Roman';

       a.FontSize = 30;

       set(gca, 'FontSize', 30, 'FontName','Times New
Roman');

       colormap(jet)
```

```
        New_A=pcdenoise(pointCloud(new_A{1, 1}));
        c=New_A.Location;
        d=B;
        pcshow(pointCloud(c))
        hold on
        %figure
        pcshow(pointCloud(d))



        sur_area_1=area_convhll(c);
        hold on


        sur_area_2=area_convhll(d);
        percentage_of_comple=
min(100,round(sur_area_1/sur_area_2,2)*100);
        if k>1


percentage_of_completion=max(percentage_of_comple,cell2
mat(recognition{1,1}(k,j+1)));
        else


percentage_of_completion=percentage_of_comple;


        end
```

```
        if j>1 && (cell2mat(recognition{1,1}(k,j))>
percentage_of_completion)


recognition{1,1}(k,j+1)=recognition{1,1}(k,j);

        else


recognition{1,1}(k,j+1)=mat2cell(percentage_of_completi
on,1);

        end




        %       pcshow(pcdenoise(pointCloud(New_A{1,
1})))

    else

        if j==1

            if k>1



percentage_of_completion=max(0,cell2mat(recognition{1,1
}(k,j+1)));

            else

                percentage_of_completion=0;


            end



recognition{1,1}(k,j+1)=mat2cell(percentage_of_completi
on,1);
```

```
            else

     recognition{1,1}(k,j+1)=recognition{1,1}(k,j);

            end

        end


        X=D(k,:);

        Y=X(~isnan(X));


        for m =1:length(Y)

            if cell2mat(recognition{1,1}(k,j+1))>80 &&
     isempty(Y)==0

                recognition{1,1}{Y(m),j+1}=100;

            end

        end

        for i = 1:length(recognition{1,1}(:,j+1))

            s=size(cell2mat(recognition{1,1}(i,j+1)));

            if s(1)==0

                recognition{1,1}(i,j+1) = mat2cell(0,1);

            end

        end

    end

end
```

```
toc;
```